博士論文

Development of gas fermentation process with metabolically engineered *Moorella thermoacetica*

(*Moorella thermoacetica* 代謝改変株を用いたガス発酵プロセスの開発)

Kaisei Takemura

Program of Biotechnology

Graduate School of Integrated Sciences for Life

Hiroshima University

Contents

参考論文

1. **Takemura K***, Kato J*, Kato S, Fujii T, Wada K, Iwasaki Y, Aoi Y, Matsushika A, Murakami K, Nakashimada Y. Autotrophic growth and ethanol production enabled by diverting acetate flux in the metabolically engineered *Moorella thermoacetica*. J Biosci Bioeng. 2021 Dec;132(6):569-574. doi: 10.1016/j.jbiosc.2021.08.005. *: equally contributed.

2. Kato J*, **Takemura K***, Kato S, Fujii T, Wada K, Iwasaki Y, Aoi Y, Matsushika A, Murakami K, Nakashimada Y. Metabolic engineering of *Moorella thermoacetica* for thermophilic bioconversion of gaseous substrates to a volatile chemical. AMB Express. 2021 Apr 23;11(1):59. doi: 10.1186/s13568-021-01220-w. *: equally contributed.

関連論文

1. Kobayashi S*, Kato J*, Wada K, **Takemura K**, Kato S, Fujii T, Iwasaki Y, Aoi Y, Morita T, Matsushika A, Murakami K, Nakashimada Y. Reversible Hydrogenase Activity Confers Flexibility to Balance Intracellular Redox in *Moorella thermoacetica*. Front Microbiol. 2022 May 12;13:897066. doi: 10.3389/fmicb.2022.897066. PMID: 35633713; PMCID: PMC9133594. *: equally contributed.

Chapter 1

Chapter 1. Introduction

1.1 Gas fermentation as a key technology for a sustainable society.

Most commodity chemicals and fuels used in our life are derived exclusively from fossil resources, such as oil, natural gas, and coal. However, our life as dependent on these resources is not sustainable because they are limited. In addition, since the consumption of fossil resources emits carbon dioxide (CO_2) which is a cause of global warming, the climate crisis is accelerated. Therefore, in order to make our life sustainable and moderate climate change, there is an immediate need to build a carbon-recycling society that is not dependent on fossil resources.

One renewable, non-fossil-derived source for chemicals and fuels is biomass. Biomass has been used after its conversion to sugars, as exemplified by the fermentation production of ethanol by yeast [1]. In particular, fermentation production from sugars derived from lignocellulosic biomass has been well studied because it does not compete with the food supply [2]. In general, lignocellulose cannot be utilized by microorganisms for fermentation as is because of its robust structure of cellulose, hemicellulose, and lignin intertwined with each other. To break the robust structure and convert polysaccharides into fermentable monosaccharides, multiple pretreatment and hydrolysis steps are necessary [3]. The pretreatments and steps include ionic liquid extraction, ammonia fiber expansion, steam explosion, and dilute acid and enzymatic hydrolysis [3; 4]. However, these pretreatments and steps are considered as expensive methods [5]. In addition, a single method may not always be efficient, and in such cases, it may be necessary to combine several methods. Despite efforts to convert such lignocellulosic biomass to fermentable monosaccharide, lignin, which can account for up to 40 % of plant biomass,

cannot be converted to it [6; 7].

Gas fermentation is a technology for producing commodity chemicals from gaseous substrates such as hydrogen (H_2), carbon monoxide (CO), and CO_2 [8; 9] (Fig. 1-1). The mixture of these gases is called synthesis gas or syngas. The syngas can be obtained by gasifying biomass. Since biomass gasification enables the use of nearly all available carbon in biomass including lignin that is otherwise inaccessible, gas fermentation has an advantage compared to sugar and cellulosic fermentation. The gasification also allows for bypassing the expense and inefficiency of pretreatment in biomass saccharification [8]. Beyond biomass, other organic materials that can be used as feedstock for gasification include municipal solid waste and organic industrial waste. In addition, off-gases from industrial processes, such as reformed biogas and steel production, can serve as direct substrates for gas fermentation [9; 10; 11]. Moreover, H_2 and CO, the energy source in gas fermentation, can be supplied by the electrolysis of water (H_2 generation) and/or CO_2 (CO generation). If the electricity used for electrolysis of water and CO_2 is supplemented by renewable energy sources such as solar and wind power, extra CO_2 emissions can be reduced (Fig 1-1). While the technologies to convert CO_2 to CO are still in the pre-commercialization stage, the technologies to convert water to H_2 using renewable energy have already been scaled up and are available commercially [9]. Therefore, gas fermentation is a technology that contributes to building a sustainable and carbon-recycling society.

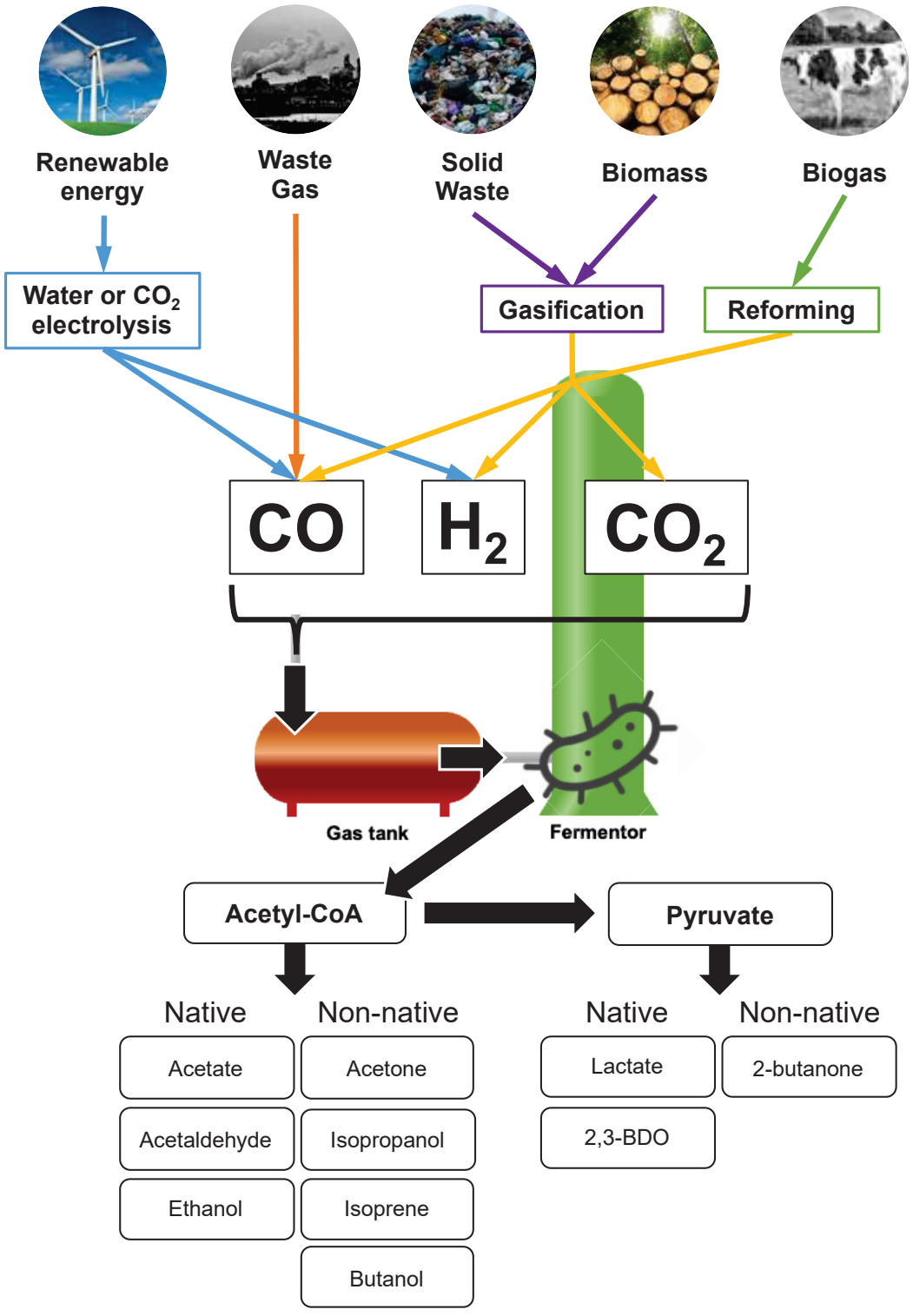

Fig. 1-1 Overview of feedstock and chemical options in gas fermentation. Non-native chemicals are those that can be generated with genetically engineered microorganisms. 2,3-BDO, 2,3-butanediol. This figure is created in reference to Figure 1 in [9].

1.2 Acetogen is a catalyst in gas fermentation.

It is well known that many organisms can convert inorganic carbon into organic materials [12]. The most common example is plant photosynthesis, but other eukaryotes, archaea, and bacteria can also utilize inorganic carbon. Among the range of autotrophic organisms, anaerobic acetogens are particularly attractive because they can utilize a pathway called the Wood-Ljungdahl pathway (WLP), which is the most efficient of the known CO_2 fixation pathways and does not require light as an energy source to fix CO_2 [13]. Fermentation processes without light offer the important advantage of being easier to scale up compared to fermentation processes with light. Table 1-1 provides an overview of the most noteworthy acetogenic species. The detailed mechanism and enzymes of the WLP have been described in several reviews [14; 15; 16; 17]. Briefly, WLP is a pathway that generates acetyl-CoA from inorganic carbon and consists of two separate branches, a methyl branch and a carbonyl branch (Fig. 1-2). In the methyl branch, the first reaction is the reduction of CO_2 to formate. Next, the formyl group of formate combines with tetrahydrofolate (THF) consuming ATP, and formyl-THF is formed. Methenyl-THF is obtained due to the separation of H_2O from formyl-THF. Then, methenyl-THF is reduced to methyl-THF via methylene-THF. The methyl group of methyl-THF is transferred to a corrinoid iron-sulfur protein (CoFeSP) by methyltransferase, resulting in generating methyl-CoFeSP. In the carbonyl branch, CO_2 is reduced to CO due to CO dehydrogenase/acetyl-CoA synthase (CODH/ACS). This enzyme also catalyzes the synthesis of acetyl-CoA using methyl-CoFeSP in the methyl branch, CO in the carbonyl branch, and CoA. After the synthesis of acetyl-CoA, it is assimilated or catabolized. Acetyl-CoA entering the catabolic pathway is converted to acetate via acetyl phosphate by phosphotransacetylase (PTA) and acetate kinase. During the acetate kinase reaction, 1

mole of ATP is generated by substrate-level phosphorylation (SLP). On the other hand, 1 mole of ATP is required for the binding of the formyl group of formate to THF. Therefore, the net synthesis of ATP by SLP is zero, suggesting that acetogens have other mechanisms for ATP synthesis. It is known that acetogens produce ATP by chemiosmotic ion gradient-driven phosphorylation (IGP) in addition to SLP under autotrophic conditions (Fig. 1-3 A and B). The IGP drives with a proton (H^+) or sodium ion (Na^+) gradient across the cellular membrane. The ion gradient is formed by a membrane-binding enzyme that oxidizes a reduced ferredoxin (Fd^{2-}) when transferring ions. Therefore, the level of Fd^{2-} is a key factor for ATP production by IGP. Fd^{2-} productivity is different when H_2 or CO is used as the energy source in gas fermentation, resulting in changing the ATP productivity by IGP. In *M. thermoacetica*, the supply of Fd^{2-} to an energy-converting hydrogenase (Ech) complex, which oxidizes Fd^{2-} to generate an H^+ gradient across the membrane, is 2 mol when H_2 is a sole energy source, while 6 mol when CO is a sole energy source (Fig. 1-3 A and B). ATP yield for oxidizing Fd^{2-} by Ech complex is estimated to be 0.25 mol-ATP/mol-Fd^{2-} [17]. ATP production by IGP when CO and H_2 are used as the energy source is 1.5 and 0.5 mol-ATP/mol-acetate, respectively. Therefore, ATP productivity is more efficient with CO than with H_2.

Table 1-1 Overview of the most noteworthy acetogenic species.

Strains	T_{opt} [°C]	Substrates	Product(s)	References
Mesophilic acetogens				
Acetobacterium woodii	30	H_2-CO_2 CO	Acetate	[18]
Clostridium aceticum	30	H_2-CO_2 CO	Acetate	[19; 20]
Clostridium autoethanogenum	37	H_2-CO_2 CO	Acetate, Ethanol, 2,3-butanediol, Lactate	[21; 22]
Clostridium ljungdahlii	37	H_2-CO_2 CO	Acetate, Ethanol, 2,3-butanediol, Lactate	[22; 23; 24]
Thermophilic acetogens				
Moorella thermoacetica	55	H_2-CO_2 CO	Acetate	[25; 26]
Moorella thermoautotrophica	58	H_2-CO_2 CO	Acetate	[27]
Thermoanaerobacter kivui	66	H_2-CO_2 CO	Acetate	[28; 29; 30]

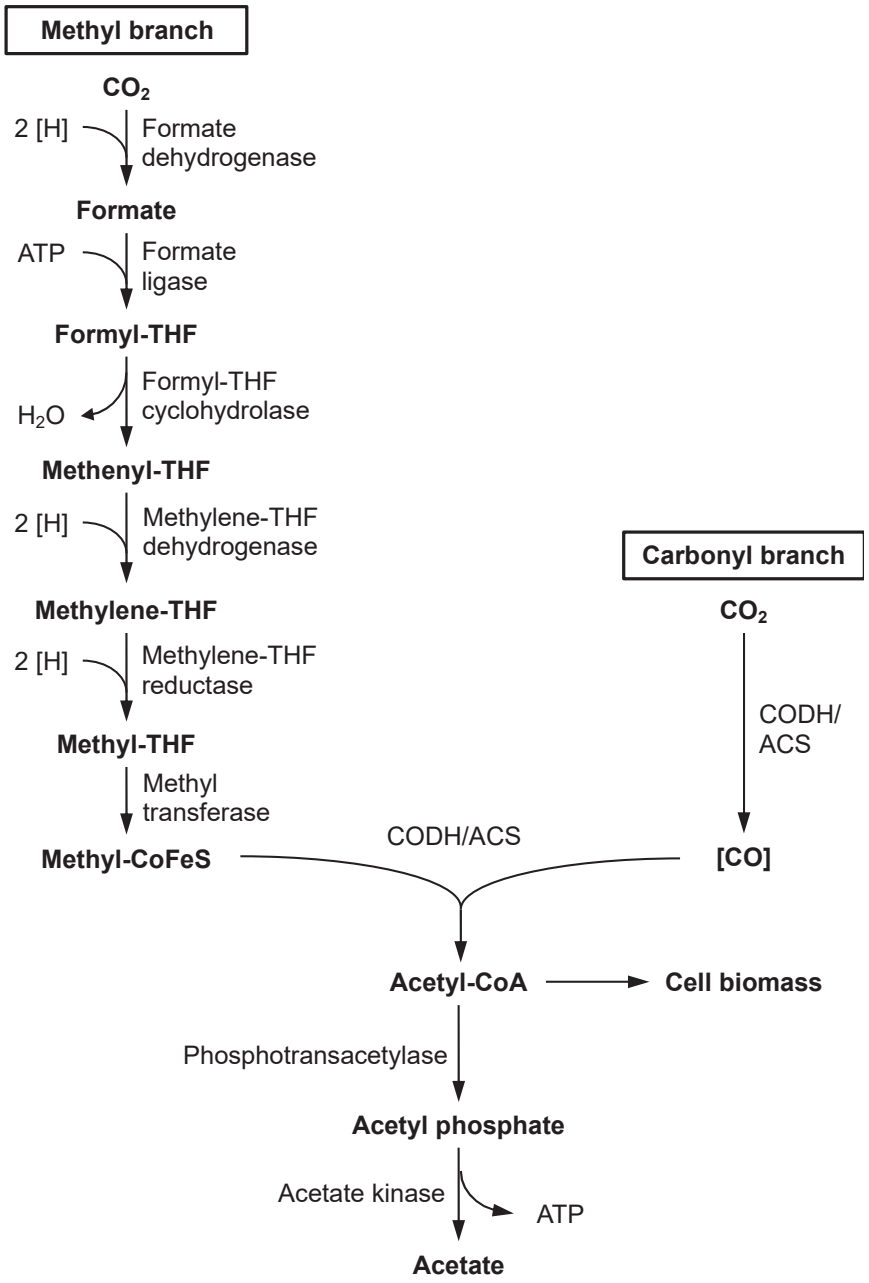

Fig. 1-2 Overview of Wood-Ljungdahl pathway (WLP). Each CO_2 is converted to a methyl-CoFeS in the methyl branch and an enzyme-bound CO in the carbonyl branch. The methyl and the CO group are combined by the CODH/ACS and further converted to acetate via acetyl phosphate. [H], reducing equivalent; THF, tetrahydrofolate; CoFeS, corrinoid-iron-sulfur protein; CODH/ACS, carbon monoxide dehydrogenase/acetyl-CoA synthase.

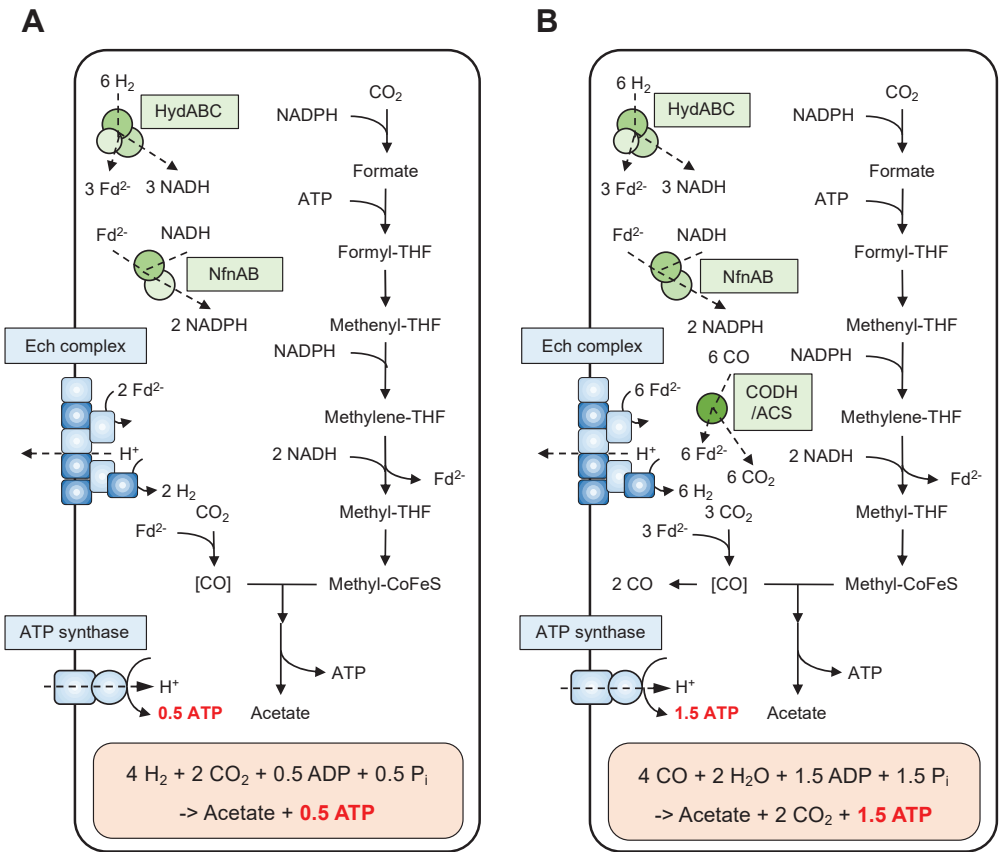

Fig. 1-3 Bioenergetics of acetate formation from (A) H_2-CO_2 and (B) CO-CO_2 in *M. thermoacetica*. (A) In H_2-CO_2 condition, the reducing equivalents to supply WLP are provided by an H_2-oxidizing, electron-bifurcating hydrogenase (HydABC) which reduces Fd and NAD^+, and by an electron-bifurcating transhydrogenase (NfnAB) which reduces $NADP^+$ with Fd^{2-} and NADH as the electron donor. (B) In CO-CO_2 condition, the reducing equivalents to supply WLP are provided by the CO-oxidizing CODH/ACS which produces Fd^{2-} and CO_2. Excess Fd^{2-} is oxidized by the Ech complex which forms H_2 and H^+ is exported to form H^+ gradient across the cell membrane. The gradient drives ATP synthesis by the H^+-dependent ATP synthase. In total, 0.5 ATP from H_2-CO_2 and 1.5 ATP from CO-CO_2 can be synthesized per acetate formation. CODH/ACS, CO dehydrogenase/acetyl-CoA synthase; THF, tetrahydrofolate; CoFeS, corrinoid-iron-sulfur protein. This figure is created in reference to Figure 4 in [31].

1.3 Expanding the product diversity in gas fermentation by discovering new acetogens and advancing genetic engineering tools.

Acetogens, as their name suggests, are often thought to produce only acetate from gaseous substrates. However, it has been reported that several acetogens produce compounds other than acetate as native products (Fig. 1-1 & Table 1-1). *C. autoethanogenum* and *C. ljungdahlii*, mesophilic acetogen, can produce ethanol, 2,3-butanediol, and lactate from gaseous substrates in addition to acetate. Sakai et al reported that *Moorella* sp. HUC22-1 is a thermophilic acetogen that produces acetate and ethanol from H_2 and CO_2 [32]. Furthermore, advancing genetic engineering tools have allowed for further expansion of the product diversity beyond native products to a range of higher-value fuels and commodity chemicals. The expanding product diversities with genetically engineered acetogens are summarized in Table 1-2. The first demonstration that acetogens can be genetically modified was reported in 2010 [24]. The study showed that *C. ljungdhalii* could produce butanol, a non-native product, from gaseous substrates by metabolic engineering. Since this report, the genetic toolboxes of mesophilic acetogens have advanced significantly. Genetic engineering of acetogens has enabled producing some non-native products, including industrially important alcohols, ketones, and dienes from gaseous substrates (Table 1-2). In thermophilic acetogens, available genetic engineering tools were developed for *M. thermoacetica* and *T. kivui* which are well-studied [33; 34]. Especially in *M. thermoacetica*, non-native products, lactate and ethanol, were successfully produced from monosaccharides with metabolically engineered strain [33; 35]. In addition, these productivities from monosaccharides were allowed to enhance by downregulating the expression of PTA related to converting acetyl-CoA to acetate [35; 36].

Table 1-2 Summary of the expanding product diversity with genetically engineered acetogens.

Strains	T_{opt} [°C]	Target product	Substrates	References
A. woodii	30	Acetone	Syngas	[37]
C. aceticum	30	Acetone	Syngas	[38]
C. autoethanogenum	37	2-Butanone	Steel mill gas, Syngas	[39]
		Acetone	Steel mill gas, Syngas	[40; 41]
		Isopropanol	Steel mill gas, Syngas	[40; 41]
		3-hydroxypropionate	Steel mill gas, H_2-CO_2	[42]
		Butyl butyrate	Steel mill gas	[43]
		Mevalonate	Steel mill gas, Syngas	[44]
		Isoprene	Steel mill gas, Syngas	[44]
C. ljungdahlii	37	Butanol	Syngas	[24]
		Acetone	CO	[45]
		Butyrate	H_2-CO_2	[46]
		Mevalonate	Syngas	[47]
		Isoprene	Syngas	[47]
		Isopropanol	CO	[48]
		3-hydroxypropionate	CO	[48]
M. thermoacetica	55	Lactate	Fructose	[33]
		Ethanol	Fructose	[35]

1.4 Advantages and challenges of gas fermentation by thermophilic acetogens. compared to mesophiles, and purposes of this study.

Gas fermentation by thermophilic acetogens may be advantageous compared to mesophiles. Advantages include a lower contamination risk of other microorganisms, and higher metabolic and diffusion rates [49; 50]. A most important advantage is that process heat can be used to culture thermophilic bacteria, thus reducing the cooling energy and cost required in the mesophilic fermentation systems. For example, if off-gases from steel mills are considered gas resources for fermentations, the heat from the gas stream could be used as fuel for the high-temperature fermenter. Moreover, one potential application is the fermentation system which involves simultaneously fermenting volatile chemicals and collecting them by distillation [51]. The fermentation systems allow for the reduction of steps and costs to purify target chemicals compared to the conventional fermentation processes with mesophilic microorganisms. In addition, the fermentation systems also permit maintaining low concentrations of fermentation products and preventing the exposure of bacteria to the chemicals that inhibit bacterial growth and metabolism.

On the other hand, while there have been many reports of improving the productivity of commodity chemicals and diversifying products by metabolic engineering in mesophilic acetogens under autotrophic conditions, in thermophiles, there have been only reports of heterotrophic conditions, and none under autotrophic conditions (Table 1-2). Understandably, there has also been no report on the gas fermentation process with the metabolically engineered thermophilic acetogens. Therefore, this study aimed to develop a technology for producing commodity chemicals from gaseous substrates with metabolically engineered thermophilic acetogens.

Chapter 2

Chapter 2. Ethanol production from gaseous substrates by metabolically engineered *Moorella thermoacetica*（参考論文 1）

2.1 Introduction

Genetic modification of thermophilic acetogen, *Moorella thermoacetica*, was first reported by Kita et al. in 2013 [33]. To engineer the ethanol-producing *M. thermoacetica*, Rahayu et al. metabolically engineered *M. thermoacetica* by using the genetic modification method [35]. In the previous study, it was shown that *M. thermoacetica* has two genes that encode phosphotransacetylase (PTA), which converts acetyl-CoA to acetyl-phosphate [52; 53], and ATP is generated by substrate-level phosphorylation (SLP) when the acetyl-phosphate is converted to acetate by acetate kinase. To engineer the ethanol-producing *M. thermoacetica*, Rahayu et al. deleted one or both PTA genes, *pduL1* and *pduL2*, and introduced an extra copy of the aldehyde dehydrogenase gene, *aldh* into the chromosome (Fig. 2-1 A and B). The strains are called Mt-Δ*pduL2*::*aldh* and Mt-Δ*pduL1*Δ*pduL2*::*aldh*. In these strains, ethanol is produced from acetyl-CoA via acetaldehyde by Aldh and endogenous alcohol dehydrogenase (Adh). Since almost all the acetyl-CoA is converted to acetate due to a strong enzymatic activity of PduL2, the *pduL2* gene must be deleted for ethanol production [35]. The Mt-Δ*pduL2*::*aldh* strain produced ethanol and acetate from fructose. The acetate production was induced by the remaining activity of PTA derived from PduL1. The Mt-Δ*pduL1*Δ*pduL2*::*aldh* strain produced more ethanol from monosaccharides. Since the autotrophic growth of both ethanol-producing strains has not been well studied, in this chapter, both strains were cultured under several autotrophic conditions for evaluating autotrophic growth and ethanol production.

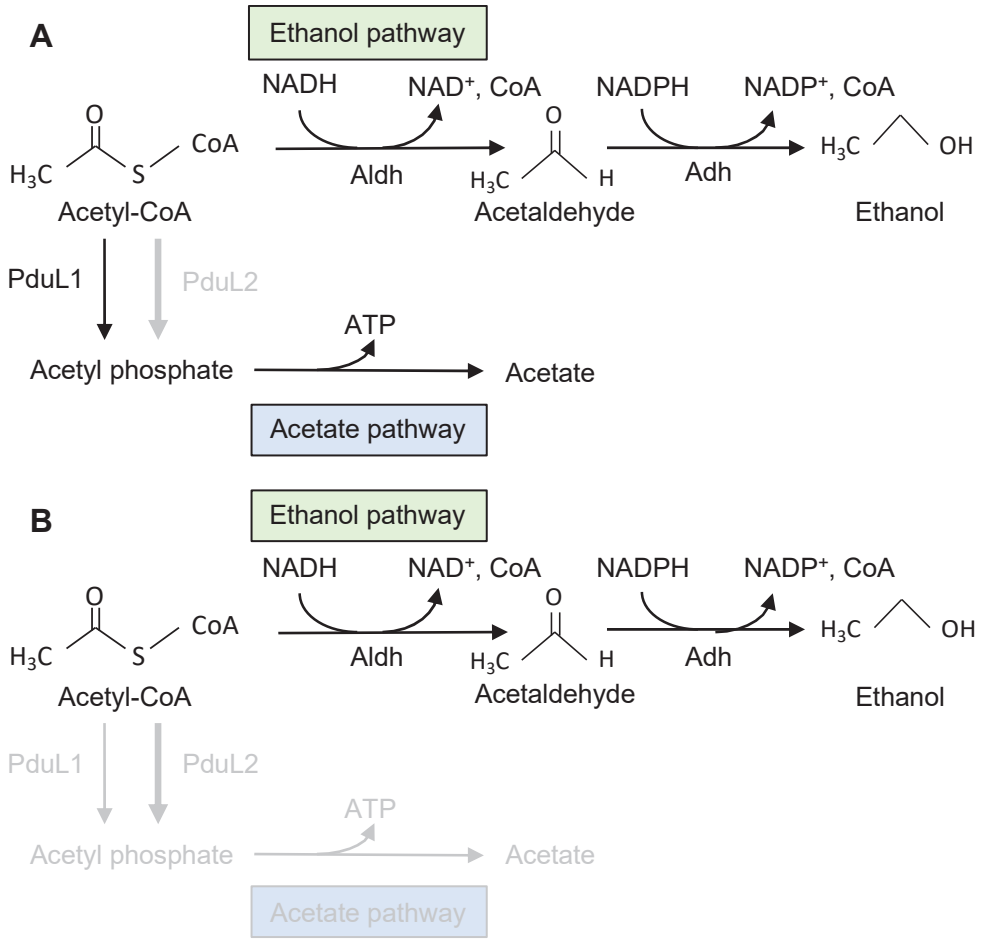

Fig. 2-1 Scheme of production of ethanol or acetate from acetyl-CoA by the two ethanol-producing strains: **(A)** Mt-Δ*pduL2::aldh* strain; **(B)** Mt-Δ*pduL1*Δ*pduL2::aldh* strain. Acetyl-CoA is converted to acetate via acetyl phosphate or is converted to ethanol via acetaldehyde. NADH is consumed when acetaldehyde is produced from acetyl-CoA, then, to produce ethanol, NADPH is consumed. Aldh, Aldehyde dehydrogenase; Adh, Alcohol dehydrogenase; PduL1 and PduL2, Phosphotransacetylase. The gray or black arrows indicate the non-functional and functional pathways, respectively.

2.2 Materials and Methods

2.2.1 Bacterial strains and growth conditions

The strains used in this study were shown in Table 2-1. The metabolically engineered strains to produce ethanol derived from *M. thermoacetica* ATCC39073 have been reported [35]. The basal medium in this study was a modified version of ATCC1754 PETC medium [54] and prepared as follows: the basal medium contained 1.0 g of NH_4Cl, 0.1 g of KCl, 0.2 g of $MgSO_4 \cdot 7H_2O$, 0.8 g of NaCl, 0.1 g of KH_2PO_4, 0.02 g of $CaCl_2 \cdot 2H_2O$, 2.0 g of $NaHCO_3$, 10 ml of trace elements [55], 10 ml of Wolfe's vitamin solution [56], and 1.0 mg of resazurin per liter of deionized water. The pH of the medium was adjusted to 6.9 with hydrochloric acid (HCl). To remove oxygen, the medium was prepared by boiling and cooling the medium under nitrogen (N_2)-CO_2 (=80:20) gas. The medium was dispensed to 45 ml per serum bottle (125 ml) under N_2-CO_2 gas. The serum bottles were subsequently crimp sealed and autoclaved (121 °C, 15 min). Before starting the culture, yeast extract and L-Cysteine·HCl·H_2O were added to 1.0 g/L and 1.2 g/L, respectively. L-Cysteine·HCl·H_2O was added as a reducing agent to remove oxygen in the serum bottles. To add the gas substrates, the headspace of the serum bottles was replaced by N_2 gas at the atmospheric pressure, followed by supplementation of H_2-CO_2 (=80:20) mixed gas at 0.1 MPa or CO gas at 0.04 MPa. Additional H_2 gas at 0.04 MPa was added when necessary. The final volume was reached 50 ml upon inoculation. Cells were grown at 55℃ on no shaking and shaken at the speed of 180 rpm.

Table 2-1 Strains used in this study

Strains	Description	Reference
ATCC 39073	Wild strain.	ATCC
Mt-Δ*pduL2*::*aldh*	*pyrF* and *aldh* were introduced to the *pduL2* region and *pduL2* was disrupted. *pyrF* and *aldh* were derived from ATCC39073. The expression of *aldh* was driven by glyceraldehyde 3-phosphate dehydrogenase (G3PD) promoter.	[35]
Mt-Δ*pduL1*Δ*pduL2*::*aldh*	*kanR* (kanamycin resistance gene) was introduced to *pduL1* of Mt-Δ*pduL2*::*aldh* and *pduL1* was disrupted.	[35]

2.2.2 Analytical methods

A portion of the culture medium was sampled and analyzed at each time point. The dry cell weight was calculated from the optical density at 600 nm using the following formula (1 g [dry cell weight]/litter = 0.383 optical density at 600 nm) [52].

Acetate, ethanol, and formate were measured and quantified by high-performance liquid chromatography (HPLC) (LC-2000 Plus HPLC; Jasco, Tokyo, Japan) with a refractive index detector (RI-2031 Plus; Jasco), Shodex RSpak KC-811 column (Showa Denko, Kanagawa, Japan), and a guard column (Shodex RSpak KC-G; Showa Denko). The column oven temperature was set at 60 °C. The mobile phase was ultrapure water containing 0.1 % (vol/vol) phosphoric acid. The flow rate was 0.7 ml/min. The internal standard was crotonate [57].

To analyze the gas composition in the headspace, gas chromatography (GC-8A; Shimadzu, Kyoto, Japan) with a thermal conductivity detector and a stainless steel column packed with activated carbon. The column oven temperature was set at 90 °C. The carrier gas was argon [58]. Inorganic carbon (IC) in the culture medium was

measured and quantifies by a total organic carbon analyzer (TOC-L; Shimadzu).

The intracellular ATP levels were measured and quantified by the BacTiter-Glo™ Microbial Cell Viability Assay kit (Promega Corporation, USA) and Infinite 200 PRO multimode plate reader (Tecan Trading AG, Switzerland). The samples were collected when the growth reached the logarithmic phase. If the strain shows no growth, the samples at the same time point were used. After collecting samples, it was immediately cooled on ice. The protocol for measuring intracellular ATP in the strains and generating an ATP standard curve was performed following the manufacturer's instructions.

The ratio of NADH/ NAD^+ was determined by EnzyFluo NAD^+/NADH assay kit (BioAssay Systems, Hayward, USA). The samples were collected when the growth reached the logarithmic phase. If the strain shows no growth, the samples at the same time point were used. After collecting samples, it was immediately cooled on ice. Cells from the whole culture were collected by centrifugation (10,000 g, 4℃, 10 min), then washed with phosphate-buffered saline (pH 7.4) before the assays. The protocol for measuring NADH and NAD^+ in the strains and generating an NADH and NAD^+ standard curve was performed following the manufacturer's instruction.

2.3 Results and Discussion

2.3.1 Metabolically engineered *M. thermoacetica* strains did not grow and produce ethanol in H_2-CO_2 condition

CO_2 and H_2 are frequently used as substrates for autotrophic acetogenesis. First, to test the growth and ethanol production under autotrophic conditions, both strains were cultured in the H_2-CO_2 condition. To set up the H_2-CO_2 culture, the strains were inoculated into the basal medium with fructose and were grown until the mid-logarithmic phase. Then, the strains were transferred into the fresh medium with H_2-CO_2 in the headspace of the vial for the pre-culture. This step was performed to completely consumed fructose and to adapt the strain to the H_2-CO_2 condition. Finally, the adapted cells were inoculated into the new fresh medium supplemented with H_2-CO_2. In this condition, neither of both strains grows and ethanol production was not observed (Fig. 2-2 A and B). These results suggested that H_2-CO_2 was not a suitable substrate for growth and ethanol production for either strain. Both strains produced a small amount of formate from H_2-CO_2. Formate is the first compound to which CO_2 is reduced by formate dehydrogenase in the methyl branch of the Wood-Ljungdahl pathway (WLP) (Fig. 1-2). ATP is required to convert formate to formyl-THF by formate ligase. Therefore, the accumulation of formate suggested that the reaction of formate ligase was stopped by "ATP shortage". When the intracellular level of ATP was measured, almost no ATP was detected in both strains (Mt-Δ*pduL2::aldh* strain, Not detected; Mt-Δ*pduL1*Δ*pduL2::aldh*, 2.9 ± 2.9 nmol/g-cell). These results indicated that the metabolism was in "ATP shortage" state, even in the presence of PduL1 where ATP supplement is higher. In fact, a small amount of acetate was detected in the culture of the Mt-Δ*pduL2::aldh* strain, indicating that ATP was produced by SLP (Fig. 2-2A). The acetate production showed that acetyl-

CoA was generated from H_2-CO_2, while the amount of acetyl-CoA may be presumably not sufficient to be converted to ethanol. Since Aldh shows a higher K_m value and a lower V_{max} value than PduL1, no ethanol production from H_2-CO_2 may be due to lower enzyme activity related to ethanol production from acetyl-CoA [53; 59].

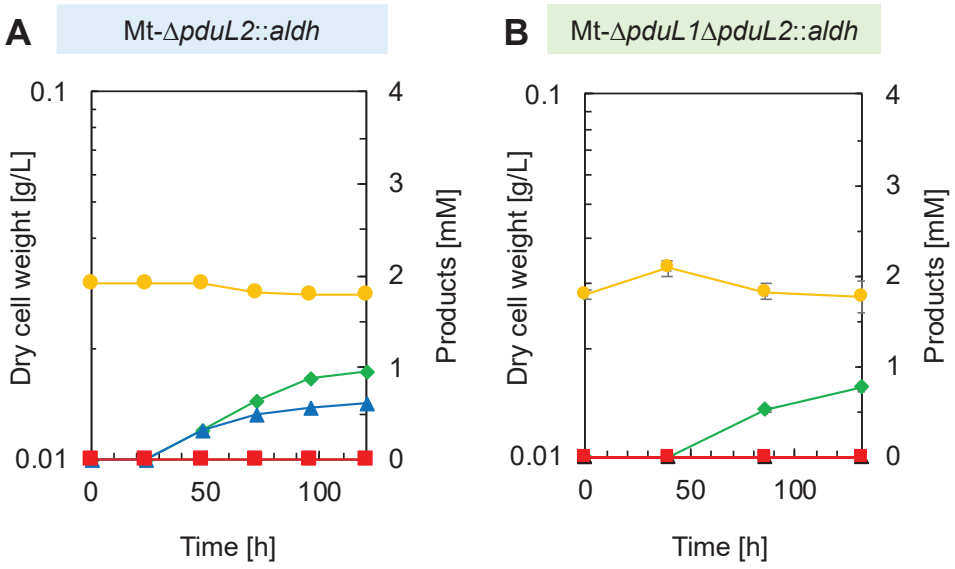

Fig. 2-2 Growth and fermentation products of the ethanol-producing strains under the H_2-CO_2 condition: **(A)** H_2-CO_2 culture of Mt-Δ*pduL2*::*aldh* strain; **(B)** H_2-CO_2 culture of Mt-Δ*pduL1*Δ*pduL2*::*aldh* strain. Symbols: ●, Dry cell weight; ■, Ethanol; ▲, Acetate; ◆, Formate. The experiment was performed in triplicates, and standard deviations (SDs) are shown by error bars. Most error bars showing a small error range overlapped with symbols of data plots.

2.3.2 Autotrophic growth and ethanol production in CO-containing gases

It was indicated that, in the H_2-CO_2 condition, the metabolism of ethanol-producing strains was in "ATP shortage" state. ATP productivity is more efficient with CO than with H_2 (Fig 1-3). Therefore, autotrophic growth and ethanol production may be possible under CO-containing conditions.

To test autotrophic growth and ethanol production from CO-containing gases, the Mt-*⊿pduL2::aldh* or Mt-Δ*pduL1*Δ*pduL2::aldh* strains were cultured in the CO-CO_2 condition. To adapt the strains to the condition, the strains were cultured with a similar method when the strains were adapted to H_2-CO_2. The gas composition was changed to CO-CO_2 from H_2-CO_2. The Mt-Δ*pduL2*::*aldh* strain grew and produced ethanol and acetate in the CO-CO_2 condition, indicating that the absolute flux of acetyl-CoA to acetate is not required for growth under this culture condition (Fig. 2-3A). On the other hand, the Mt-Δ*pduL1*Δ*pduL2*::*aldh* strain revealed almost no growth under the CO-CO_2 condition, and not only no ethanol or acetate formation was detected, but also no accumulation of formate was observed (Fig. 2-3B). In the Mt-Δ*pduL1*Δ*pduL2*::*aldh* strain, the pduL1 gene is deleted unlike in the Mt-*⊿pduL2::aldh* strain. This difference would strengthen the flow of acetyl-CoA into ethanol, resulting in ATP production by SLP being reduced and/or requiring more reducing power. Therefore, it was thought that the cause of the culture profile of the Mt-Δ*pduL1*Δ*pduL2*::*aldh* strain was "ATP shortage" or/and "redox imbalance". To investigate the cause of no ethanol production from CO-CO_2, the intracellular level of ATP and NADH/NAD^+ ratio of both strains were measured. NADH is the reducing power used by Aldh to convert acetyl-CoA to acetaldehyde (Fig. 2-1). Although the loss of ATP production was small, the NADH/NAD^+ ratio of the Mt-Δ*pduL1*Δ*pduL2*::*aldh* strain was significantly lower than that of the Mt-Δ*pduL2*::*aldh*

strain, indicating that the NADH level was poor and the metabolism was in “redox imbalanced” state (Table 2-2).

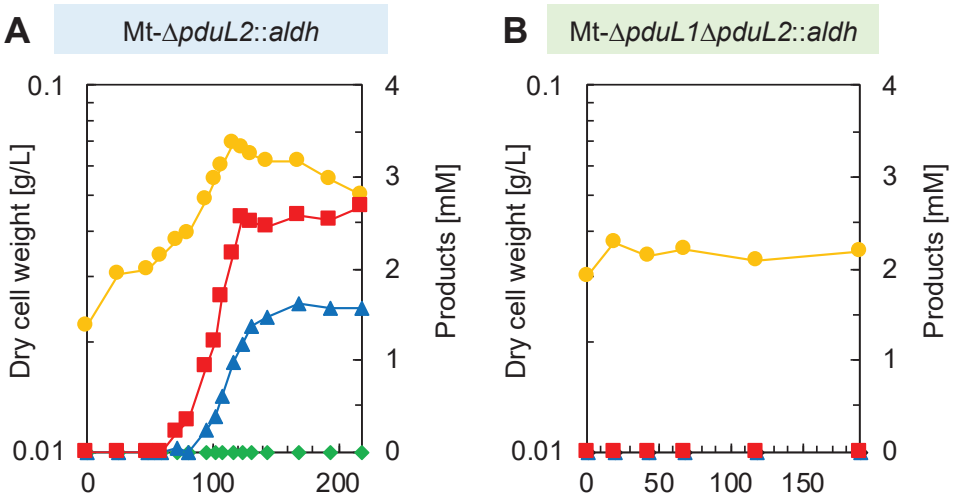

Fig. 2-3 Growth and metabolites profiles of the ethanol-producing strains under the CO-CO_2 condition: **(A)** CO-CO_2 culture of Mt-Δ*pduL2*::*aldh* strain; **(B)** CO-CO_2 culture of Mt-Δ*pduL1*Δ*pduL2*::*aldh* strain. Symbols: ●, Dry cell weight; ■, Ethanol; ▲, Acetate; ◆, Formate. The experiment was performed in triplicates, and standard deviations (SDs) are shown by error bars. Most error bars showing a small error range overlapped with symbols of data plots.

Table 2-2 Quantification of intracellular level of ATP and NADH/NAD^+ ratio in CO-CO_2 condition

Substrate	Strain	ATP nmol/g-cell	NADH/NAD^+
CO-CO_2	Mt-Δ*pduL2*::*aldh*	102.0 ± 32.8	0.34 ± 0.13
	Mt-Δ*pduL1*Δ*pduL2*::*aldh*	77.3 ± 6.7	0.03 ± 0.01

When using CO as a sole energy source or CO and H_2 as energy sources, acetyl-CoA is produced as follows:

$$4CO + H_2O + CoA \rightarrow Acetyl\text{-}CoA + 2CO_2$$

$$2CO + 2H_2 + CoA \rightarrow Acetyl\text{-}CoA + H_2O$$

The theoretical yields of acetyl-CoA per CO without or with H_2 are 0.25 and 0.50 mol-acetyl-CoA/mol-CO, respectively, indicating that if the same amount of CO is consumed, more acetyl-CoA is generated with H_2. Since ethanol is produced from acetyl-CoA, the increase in acetyl-CoA may result in increasing ethanol production. In the case of gas fermentation with *C. autoethanogenum*, ethanol production was increased by H_2 supplementation [60]. To investigate the effect of the addition of H_2 on ethanol productivity from gaseous substrates, the Mt-Δ*pduL2*::*aldh* strain was cultured under the H_2-CO-CO_2 condition (Fig. 2-4A). The strain grew and produced ethanol and acetate in the condition. The cell biomass was similar between the H_2-CO-CO_2 and CO-CO_2 conditions, indicating that the total ATP level was similar. Although the final ethanol production was also similar, the final acetate production was significantly higher in the H_2-CO-CO_2 condition than in the CO-CO_2 condition. The high acetate production indicated that acetyl-CoA was preferentially converted into acetate rather than ethanol and more ATP was provided by SLP. Formate was also detected in the late culture phase under the H_2-CO-CO_2 condition. CO was not detected at the endpoint of the culture, indicating that the composition of the gas substrate was changed from the H_2-CO-CO_2 mixture to the H_2-CO_2 mixture during the culture. Therefore, this formate accumulation was most likely due to the ATP limitation as in the H_2-CO_2 culture. The fermentative characteristics of the Mt-*ΔpduL2*::*aldh* strain in the CO-H_2-CO_2 and CO-CO_2 conditions are shown in Table 2-3. The sum of ethanol and acetate yield for the consumed CO was

higher with H_2 addition than without H_2 addition. Since ethanol and acetate were generated from acetyl-CoA, this result indicated that the addition of H_2 increased acetyl-CoA yield per CO, which is consistent with the above estimate.

Despite the acetyl-CoA level being increased by H_2 supplementation, ethanol production was not affected. On the other hand, the amount of acetate was higher than without H_2. This increase showed that ATP production by SLP was increased. The amount of the cell biomass with or without H_2 was similar, indicating that the same amount of ATP was generated. In *M. thermoacetica* under autotrophic conditions, two ATP synthesis mechanisms, which are SLP and chemiosmotic ion (proton) gradient-driven phosphorylation (IGP), are functional (Fig. 1-3). In the H_2-CO-CO_2 condition compared to the CO-CO_2 condition, while ATP production by SLP was increased, total ATP production was similar, indicating that ATP production by IGP was reduced by the addition of H_2. The cause of the decrease in IGP due to H_2 supplementation can be explained as follows. Ion (proton) export, which leads to ATP synthesis by ATP synthase, is driven by the reaction of Ech complex according to the formula:

$$2Fd^{2-} + 4H^+ \rightarrow 2Fd + 2H_2$$

Therefore,

$$\Delta G' = \Delta G_0' + RT \ln[Fd][H_2]/ [Fd^{2-}][H^+]$$

This formula indicates that $\Delta G'$ increases when the H_2 concentration increases, becoming more difficult to export protons outside the cell. In this scenario, if the H_2 level is high, ATP production by IGP is difficult. The enhancement of SLP coupled to acetate synthesis from acetyl-CoA may be to compensate for this low IGP, resulting in not enhancing ethanol productivity from acetyl-CoA. On the other hand, in *C. autoethanogenum*, the ethanol production is increased by H_2 supplementation. Since the strain uses the Rnf

complex, which requires NAD^+ as an electron acceptor to export protons [61], H_2 supplementation would not directly affect proton export in such a way, and the provided reducing power by H_2 could be used for ethanol production. This result suggests that changing the gas composition could be a strategy to reduce acetate as the byproduct for industrial applications.

The Mt-Δ*pduL1*Δ*pduL2*::*aldh* strain also was cultured under the H_2-CO-CO_2 condition, but the strain did not grow and produce any metabolites (Fig. 2-4B). Presumably, the redox state is unbalanced as in the CO-CO_2 condition.

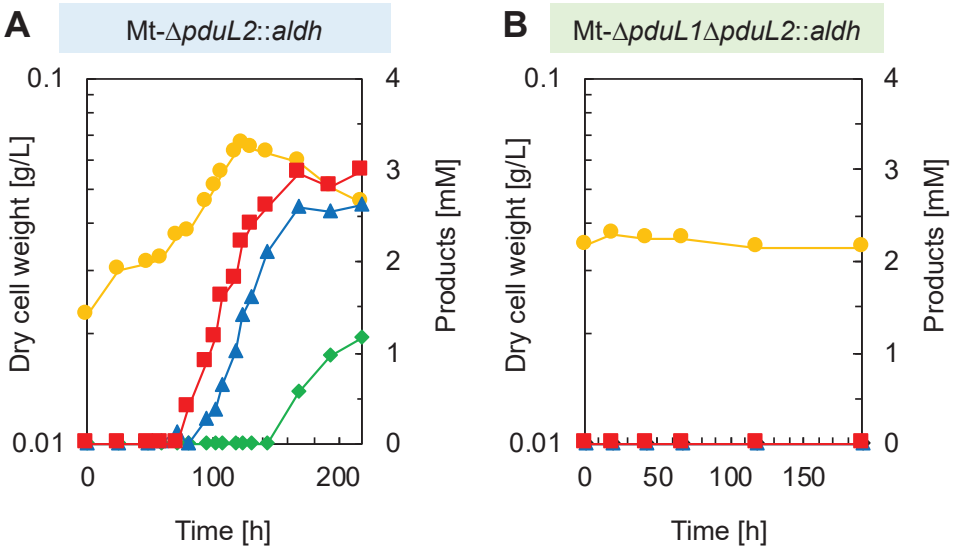

Fig. 2-4 Growth and metabolites profiles of the ethanol-producing strains under the CO-CO_2 condition: **(A)** H_2-CO-CO_2 culture of Mt-Δ*pduL2*::*aldh* strain; **(B)** H_2-CO-CO_2 culture of Mt-Δ*pduL1*Δ*pduL2*::*aldh* strain. Symbols: ●, Dry cell weight; ■, Ethanol; ▲, Acetate; ◆, Formate. The experiment was performed in triplicates, and standard deviations (SDs) are shown by error bars. Most error bars showing a small error range overlapped with symbols of data plots.

Table 2-3 Fermentation parameters for ethanol production from CO-containing gas.

Substrate	Consumed substrates		Yield for CO					Recovery	
	CO	H_2	Biomass[a]	Acetate	Ethanol	Formate	CO_2	Carbon	Electron
	mmol	mmol	mol/mol	mol/mol	mol/mol	mol/mol	mol/mol	%	%
H_2-CO-CO_2	1.17 ± 0.02	0.17 ± 0.01	0.01 ± 0.00	0.08 ± 0.00	0.10 ± 0.00	0.01 ± 0.00	0.50 ± 0.02	92.3 ± 1.8	91.4 ± 1.6
CO-CO_2	1.14 ± 0.10	N.A.[b]	0.01 ± 0.00	0.05 ± 0.00	0.09 ± 0.00	N.D.[c]	0.63 ± 0.05	99.5 ± 7.4	92.7 ± 4.9

[a] By assuming the cell composition to be $C_5H_8O_2N_1$.

[b] Not applied. [c] Not detected.

2.4 Conclusion

In this chapter, it was demonstrated for the first time that the metabolically engineered *M. thermoacetica* can produce a target chemical, ethanol, from gaseous substrates, and indicated several bottlenecks in the metabolism of metabolically engineered strains used for gas fermentation. Firstly, the two ethanol-producing strains were cultured in the H_2-CO_2 condition. Although both strains did not form the cell biomass and ethanol, the strains produced formate, which is converted to acetyl-CoA via a reaction requiring ATP in WLP. The ATP levels in both strains were measured and not detected, indicating that the metabolism was in "ATP shortage" state. To supply ATP, the strains were cultured under conditions using CO. The Mt-Δ*pduL2*::*aldh* strain grew and produce ethanol. In addition, it was found that the gas composition with CO as a sole energy source is preferable for autotrophic ethanol production. In contrast, even under the condition suitable for its autotrophic ethanol production, the Mt-Δ*pduL1*Δ*pduL2*::*aldh* strain did not grow and produce any metabolites including formate. In the comparison of the levels of several biomolecules between both strains under the CO-CO_2 condition, the $NADH/NAD^+$ ratio of the Mt-Δ*pduL1*Δ*pduL2*::*aldh* strain was significantly lower than that of the Mt-Δ*pduL2*::*aldh* strain, indicating that the metabolism was in "redox imbalance" state. Therefore, it was indicated that there are bottlenecks, "ATP shortage" and "redox imbalance", in the metabolism in metabolically engineered stains to be used for gas fermentation. When multiple issues are present, it is not easy to address individual issues. To facilitate addressing individual issues, it would be necessary to separate issues.

Chapter 3

Chapter 3. Acetone production from gaseous substrates and the effect of ATP enhancement on gas fermentation（参考論文 2）

3.1 Introduction

In chapter 2, it was indicated that the metabolism in metabolically engineered strains to be used for gas fermentation has two bottlenecks: “ATP shortage” and “redox imbalanced”. The presence of multiple issues makes it difficult to approach individual issues. One way to facilitate approaching individual issues is to separate issues. If there is a strain with introduced the metabolic pathways that do not involve redox reactions, it is considered that “redox imbalanced” could be ignored and the only issue would be “ATP shortage”.

Since the acetone biosynthesis pathway from acetyl-CoA does not require redox reactions, the redox balance would be maintained as in the acetate production of wild type. (Fig. 3-1A). Moreover, acetone is the desired compound to be produced from renewable resources because it is one of the important industrial chemicals [62; 63; 64] and, currently, is mainly produced as a co-product in the process of phenol production from unrenewable fossil resources [65]. Furthermore, since the boiling point of acetone (56 °C) is lower than the boiling point of ethanol (78 °C) and the growth temperature of *M. thermoacetica* (45-65 °C), acetone would be a more suitable chemical than ethanol for evaluating gas fermentation systems that can simultaneously collect volatile chemicals by distillation during fermentation.

Thus, in this chapter, *M. thermoacetica* was metabolically engineered to produce acetone from gaseous substrates and the effect of ATP increase on gas fermentation using an acetone-producing strain was evaluated.

3.2 Materials and Methods

3.2.1 Bacterial strains and growth conditions.

M. thermoacetica ATCC 39073 and its derivatives were used in this study. The strains used in this study were shown in Table 3-1. The basal medium in this study was a modified version of ATCC1754 PETC medium [23] and prepared as follows. The basal medium contained 1.0 g of NH_4Cl, 0.1 g of KCl, 0.2 g of $MgSO_4 \cdot 7H_2O$, 0.8 g of NaCl, 0.1 g of KH_2PO_4, 0.02 g of $CaCl_2 \cdot 2H_2O$, 2.0 g of $NaHCO_3$, 10 ml of trace elements [55], 10 mL of Wolfe's vitamin solution [55], and 1.0 mg of resazurin per liter of deionized water. The pH was adjusted to 6.9 by using hydrochloric acid (HCl). To remove oxygen, the medium was anaerobically prepared by boiling and cooling the medium under N_2-CO_2 (=80:20) mixed gas. After cooling, the medium was dispensed to 15 or 45 ml per serum bottle (125 mL) under N_2-CO_2. The serum bottles were subsequently crimp sealed and autoclaved (121 °C, 15min). Before the start of incubation, yeast extract and L-Cysteine $\cdot$ HCl $\cdot$ H_2O were added to the final concentration of 1.0 g/L and 1.2 g/L, respectively. Fructose (2.0 g/L) was added as needed. The final medium volume was adjusted to 20 or 50 mL. After replacing the headspace with N_2 gas at the atmospheric pressure, the headspace of the serum bottles was replaced by H_2-CO_2 (=80:20) mixed gas of 0.1 MPa, or CO (0.04 MPa) and additional H_2 (0.04 MPa) were added to provide gas substrates. The culture was performed at 55℃ with shaking at 180 rpm.

Table 3-1 Strains and plasmids used in this study

Strain or plasmid	Description	Source or reference
Strains		
Escherichia coli		
HST08	Cloning host	TaKaRa
TOP10	Modification host	Invitrogen
M. thermoacetica		
ATCC 39073	Wild strain	ATCC
Δ*pyrF*	*pyrF* gene was eliminated from ATCC39073	[33]
pyrF::acetone	The thermophilic acetone operon was inserted into the eliminated *pyrF* locus of Δ*pyrF* strain by using pHM17	This study
pduL2::acetone	The thermophilic acetone operon was inserted into the *pduL2* region of Δ*pyrF* strain by using pHM5. As a result, *pduL2* was deleted.	This study
Plasmids		
pBAD33	Backbone plasmid for methylation plasmids, Cm^r	[66]
pBAD-M1281	pBAD33 carrying the Moth_1671, Moth_1672, and Moth_2281, which are putative methyltransferase genes in *M. thermoacetica* ATCC39073.	[33]
pK18mob	Backbone plasmid for transformation plasmids, Km^r	[67]
pK18-ldh	A plasmid to insert Ldh (lactate dehydrogenase) gene into the *pyrF* region. The selection marker was *pyrF*.	[33]
pK18-Δ*pduL2*::*ldh*	A plasmid to introduce Ldh gene into the *pduL2* region. The selection marker is *pyrF*.	[36]
pHM17	A plasmid to insert the thermophilic acetone operon into the *pyrF* region. The selection marker is *pyrF*.	This study
pHM5	A plasmid to insert the thermophilic acetone operon into the pduL2 region. The selection marker is *pyrF*.	This study

3.2.2 The construction of plasmids

Two plasmids, pHM17 and pHM5, were constructed for inserting the thermophilic acetone operon into the *pyrF* region or *pduL2* region of *M. thermoacetica* (Table 3-1). The thermophilic acetone operon consisted of four genes which were *ctfA* (Tmel_1136) and *ctfB* (Tmel_1135) derived from *Thermosipho melanesiensis*, *thl* (TTE0549) derived from *Caldanaerobacter subterraneus* subsp. *Tengcongensis*, and *adc* (CA_P0165) derived from *C. acetobutylicum*, and the codons of these genes were optimized to express genes in *M. thermoacetica* (Fig. 3-1A). The open reading frames coding these four genes were driven by the constitutive glyceraldehyde-3-phosphate dehydrogenase (G3PD) promotor [33], and the order of the genes was decided based on the biochemical information about the enzymes: stability, activity, and complex formation [68]. An intergenic spacer with a ribosome-binding site was placed between each gene. The synthesized DNA fragments were amplified by PCR using KOD plus ver.2 (TOYOBO Co., Ltd., Osaka, Japan) and were inserted into the plasmids by In-Fusion HD cloning kit (Clontech Laboratories, TaKaRa Bio, Shiga, Japan). pK18-ldh [33] or pK18-Δ*pduL2*::*ldh* [36] was used as the template of vector for amplification (Table 3-1). The primers used in this study were listed in Table 3-2. JK50 and JK51 were used for amplifying the insert, and JK52 and JK53 were used to amplify the vector. Finally, the constructed plasmids were cloned in the *Escherichia coli* HST08 and the DNA sequences were confirmed by Sanger sequencing.

Table 3-2 PCR primers used in this study

Name	Sequence (5' to 3')
JK50	GGTGAAATAATAACTGGACGGTTGCCAAGTACCG
JK51	ATGAAAGCAGGCCGATTACTTCAGATAATCGTAGATC ACTTCGG
JK52	TCGGCCTGCTTTCATGCTTG
JK53	AGTTATTATTTCACCATCTCTATTTCCGCC
JK226	GGCCGCCGCCATTTAGCATATCAAGAG
JK227	GCCGCAAATGCTGGTAAAGGCTATC
1181-up-F	CGTTCAATAGGAAGACCACAG
1181-dw-R	GCAGTAAGCTGTATCGCAATG

3.2.3 Transformation and selection of mutants

Genetic transformation of *M. thermoacetica* was performed by following the procedure by Kita *et al* [33]. All procedures except for the growth of the cells were performed under aerobic conditions. Briefly, the *M. thermoacetica* Δ*pyrF* mutant was grown until the mid-log phase in the basal medium added with 2 g/l fructose as carbon source and 10 μg/ml of uracil instead of yeast extract, and harvested by centrifugation (5800 × g, 5 min). The cells were washed twice with 272 mM sucrose buffer and used for electroporation with methylated DNA in *E. coli* TOP10 harboring plasmid pBAD-M1281. The transformed cells were cultured at 55°C for 24-48 hours with reduced uracil concentration (1 μg/ml) and then inoculated into the agar medium without uracil supplementation in the roll tubes. The roll tubes were incubated at 55°C and the colonies were picked up for sub-cultured to confirm the insertion of the acetone operon by using PCR. JK226 and JK227 were used for amplifying the *pyrF* region and, 1181-up-F and 1181-dw-R were used for amplifying the *pduL2* region.

3.2.4 Analytical methods

A portion of the culture medium was sampled and analyzed at each time point. The dry cell weight was calculated from the optical density at 600 nm using the following formula (1 g [dry cell weight]/litter = 0.383 optical density at 600 nm) [36].

Formate, acetate, dimethyl sulfoxide (DMSO), and acetone were measured and quantified by high-performance liquid chromatography (HPLC) (LC-2000 Plus HPLC; Jasco, Tokyo, Japan) with a refractive index detector (RI-2031 Plus; Jasco), Shodex RSpak KC-811 column (Showa Denko, Kanagawa, Japan), and a guard column (Shodex RSpak KC-G; Showa Denko). The column oven temperature was set at 60 °C. The mobile phase was ultrapure water containing 0.1 % (vol/vol) phosphoric acid. The flow rate was 0.7 ml/min. The internal standard was crotonate [58].

To analyze the gas composition in the headspace, gas chromatography (GC-8A; Shimadzu, Kyoto, Japan) with a thermal conductivity detector and a stainless steel column packed with activated carbon. The column oven temperature was set at 90 °C. The carrier gas was argon [58]. Inorganic carbon (IC) in the culture medium was measured and quantifies by a total organic carbon analyzer (TOC-L; Shimadzu).

The intracellular ATP levels were measured and quantified by the BacTiter-Glo™ Microbial Cell Viability Assay kit (Promega Corporation, USA) and Infinite 200 PRO multimode plate reader (Tecan Trading AG, Switzerland). The samples were collected when the growth reached the logarithmic phase. If the strain shows no growth, the samples at the same time point were used. After collecting samples, it was immediately cooled on ice. The protocol for measuring intracellular ATP in the strains and generating an ATP standard curve was performed following the manufacturer's instructions.

The formation of dimethyl sulfide (DMS) was monitored using gas chromatography-mass spectrometry (GC-MS). Agilent GC 7890A attached with Agilent 7693A autosampler (Agilent Technologies, USA) was used as a GC system, and Agilent 7000 (Agilent Technologies, USA) was used as an MS system. GC-MS conditions were as follows: column, DB-WAX (60 m x 0.32 mm, 0.25 μm); Oven temperature, 40°C for 3 min, increased by 10℃/min to 240℃; Carrier gas, helium gas; Injection volume, 1 μl; Injection port temperature, 250℃; Transfer line temperature, 290℃; Flow rate, 12 ml/min; Split rate, 10:1; Ion source temperature, 250℃; m/z, 60-65. Dimethyl ether was used as an internal standard.

3.3 Results and Discussion

3.3.1 Design and construction of metabolically engineered thermophilic *M. thermoacetica* strains to produce acetone

M. thermoacetica is a thermophilic microorganism and the optimal temperature is 45-65 ºC. A thermophilic acetone production pathway, which functions up to 70 °C, has been proposed with enzyme candidates [68]. In this pathway, two molecules of acetyl-CoA are converted to acetoacetyl-CoA by thiolase (Thl), then it is converted to acetone via acetoacetate by CoA transferase (CtfAB) and acetoacetate decarboxylase (Adc) (Fig. 3-1A). A CoA molecule of acetoacetyl-CoA is transfered to acetate by CtfAB, and acetoacetate and acetyl-CoA are produced. Therefore, acetate is an essential compound to produce acetone in this pathway. Both acetyl-CoA and acetate, which are used in this pathway, are supplied when *M. thermoactica* metabolites sugars or gaseous substrates. These substrates are converted to acetate as the end metabolite via acetyl-CoA. Thermophilic enzymes were selected, the acetone biosynthesis operon was designed (Fig. 3-1B), and the operon was successfully introduced into the wild-type background of *M. thermoacetica* (Fig. 3-1C and E). This engineered strain was called pyrF::acetone strain. To test whether the pathway is functional in *M. thermoacetica*, the strain was cultured in the basal medium added with fructose at 55 ºC. The strain grew and produced acetone from fructose, indicating that the enzymes in the thermophilic acetone production pathway were expressed and functioned (Fig. 3-2A and B). On the other hand, a large amount of acetate was detected (about three times more than acetone) in the culture medium, indicating that acetyl-CoA mostly was not changed to acetone (Fig. 3-2B and E).

Although repressing the acetate pathway may be more effective in increasing

acetone productivity than acetate, the pathway cannot completely be repressed because acetate is a substrate in acetone production. On the other hand, since *M. thermoacetica* has two functional phosphotransacetylase (PduL1 and PduL2) related to the conversion of acetyl-CoA to acetate, disrupting one of the genes encoding the enzymes may accomplish both supplying acetate to acetone biosynthesis pathway and enhancing acetone productivity [52; 53]. PduL2 showed more than a ten-fold lower Michaelis constant (*Km* = 0.04 mM) against acetyl-CoA compared to PduL1 (*Km* = 0.49 mM) [53]. On the other hand, Thl showed a *Km* value of 0.27 mM against acetyl-CoA [69]. Since the *Km* value of PduL2 against acetyl-CoA is lower than the *Km* value of Thl, the deletion of the gene encoding the PduL2 would be effective in increasing acetone production. To test the effect of the deletion of *pduL2* on acetone productivity, *pduL2* was knocked out and acetone production was measured. The thermophilic acetone operon was introduced to replace the *pduL2* region, making it possible to delete the *pduL2* gene and introduce acetone biosynthetic genes simultaneously (Fig. 3-1D and F). This engineered strain was called pduL2::acetone strain. The pduL2::acetone strain was cultured in the basal medium with fructose. Acetate production decreased and acetone production increased significantly, resulting in 0.45 ± 0.03 mol-acetate/mol-fructose and 1.0 ± 0.02 mol-acetone/mol-fructose (Fig. 3-2C, D and E). The acetone/acetate ratio in the pduL2::acetone strain was higher than in the pyrF::acetone strain (2.23 ± 0.21 and 0.35 ± 0.03 mol-acetone/mol-acetate, respectively). Since acetone production was more predominant than acetate production, the pduL2::acetone strain is a better acetone-producing strain than the pyrF::acetone strain. One of the purposes of this chapter is to produce acetone from gaseous substrates. Thus, to test whether the acetone is produced from gaseous substrates, the pduL2::acetone strain was cultured in autotrophic conditions.

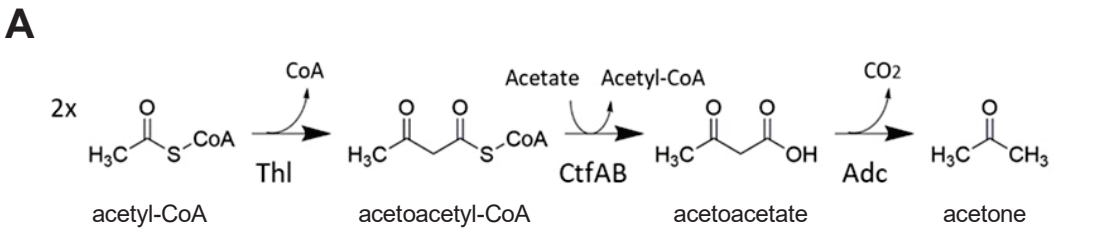
A
2x
CoA
Thl
Acetate
Acetyl-CoA
CtfAB
CO2
Adc
acetyl-CoA
acetoacetyl-CoA
acetoacetate
acetone

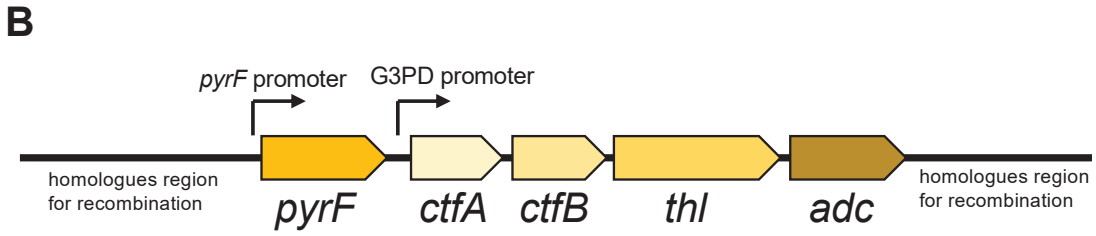
B
pyrF promoter
G3PD promoter
homologues region for recombination
pyrF
ctfA
ctfB
thl
adc
homologues region for recombination

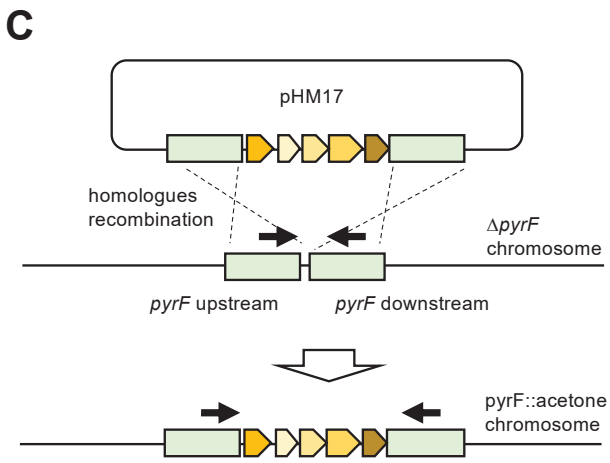
C
pHM17
homologues recombination
ΔpyrF chromosome
pyrF upstream
pyrF downstream
pyrF::acetone chromosome

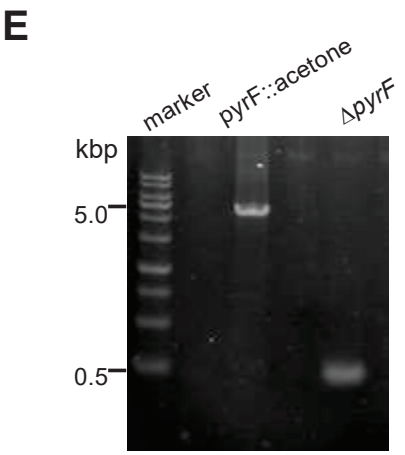
E
marker
pyrF::acetone
ΔpyrF
kbp
5.0
0.5

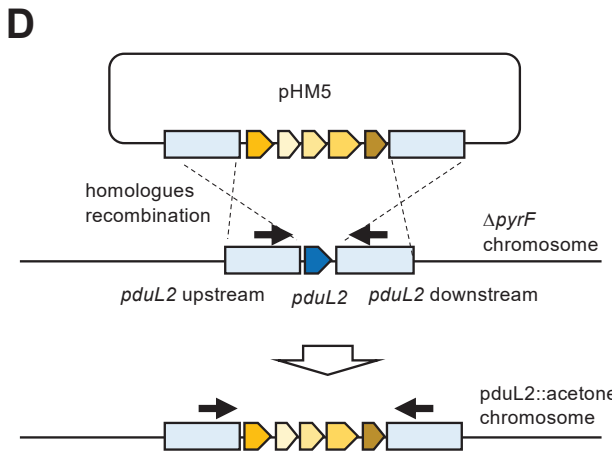
D
pHM5
homologues recombination
ΔpyrF chromosome
pduL2 upstream
pduL2
pduL2 downstream
pduL2::acetone chromosome

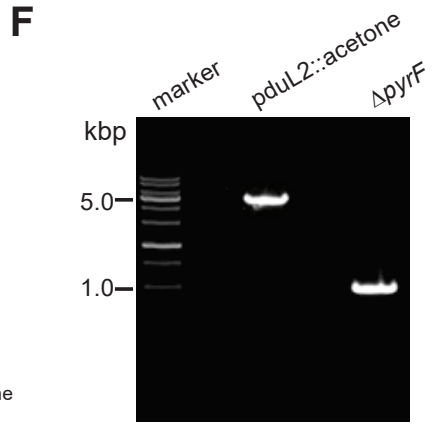
F
marker
pduL2::acetone
ΔpyrF
kbp
5.0
1.0

Fig. 3-1 Design and construction of the acetone-producing *Moorella thermoacetica* strains. **(A)** Acetone biosynthesis pathway. Thl: Thiolase, CtfAB: CoA transferase, Adc: Acetoacetate decarboxylase. **(B)** Scheme of the synthetic acetone production operon. Genes are shown with blocked arrows and promoters are shown with fine arrows. **(C)** Scheme of inserting the thermophilic acetone operon by homologous recombination into the *pyrF* region. **(D)** Scheme of inserting the thermophilic acetone operon by homologous recombination into the *pduL2* region. The light green boxes show DNA regions of *pyrF* used for recombination, and the light blue boxes show DNA regions of *pduL2* used for recombination. The line arrows show primers used for PCR. JK226 and JK227 were used for amplifying the *pyrF* region, and 1181-up-F and 1181-dw-R were used for amplifying the *pduL2* region. **(E)** Validation of the presence of the thermophilic acetone operon in the *pyrF* region. **(F)** Validation of the presence of the thermophilic acetone operon in the *pduL2* region. These regions were amplified by PCR to confirm the size shift due to the insertion. The size of the *pyrF* region was changed from 0.5 to 4.8 kb by inserting the selection marker and the thermophilic acetone operon **(E)**. Similarly, the selection marker and the thermophilic acetone operon changed the size of the *pduL2* region from 1.0 to 4.9 kb **(F)**.

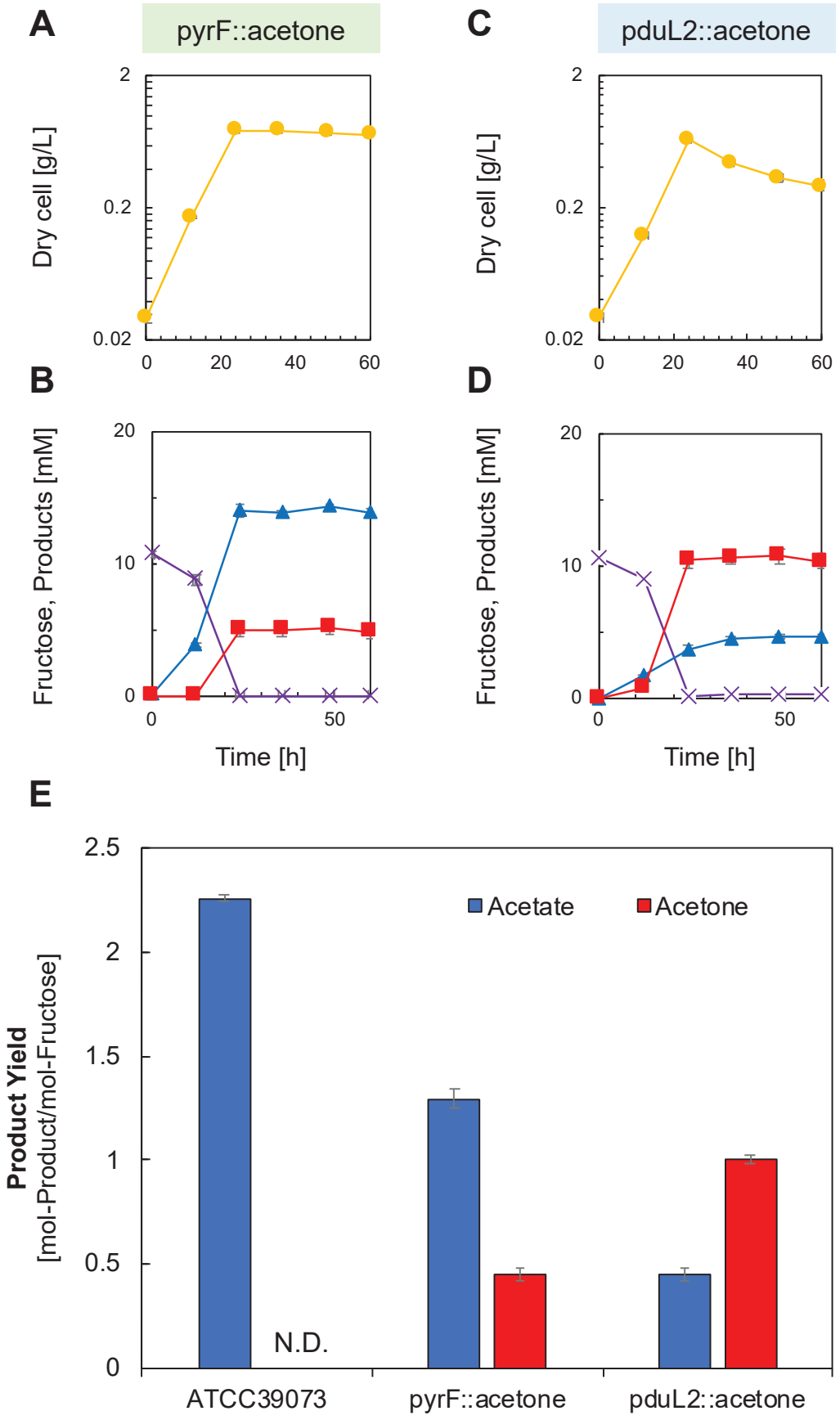
A
pyrF::acetone
C
pduL2::acetone
Dry cell [g/L]
2
0.2
0.02
0
20
40
60
B
D
Fructose, Products [mM]
20
10
0
50
Time [h]
E
Product Yield
[mol-Product/mol-Fructose]
2.5
2
1.5
1
0.5
0
Acetate
Acetone
N.D.
ATCC39073
pyrF::acetone
pduL2::acetone

Fig. 3-2 Acetone and acetate production in the condition with fructose by the metabolically engineered *Moorella thermoacetica* strains. **(A)** Dry cell weight of the pyrF::acetone. **(B)** The measured concentration of fructose and products in the culture medium by HPLC for the pyrF::acetone strain. **(C)** Dry cell weight of the pduL2::acetone strain. **(D)** The measured concentration of fructose and products in the culture medium by HPLC for the pduL2::acetone strain. Symbols: ●, Dry cell weight; ■, Acetone; ▲, Acetate; ×, Fructose. The experiment was performed in triplicates, and standard deviations (SDs) are shown by error bars. Most error bars showing a small error range overlapped with symbols of data plots. **(E)** The acetone and acetate yield for consumed fructose is shown with blue (acetone) and red (acetate) bars. The yields were calculated based on the consumed amount of fructose. The parental strain, the yields for consumed fructose of ATCC 39073 (wild strain) was shown for comparison which does not produce acetone is shown for comparison. The experiment was performed in triplicates, and standard deviations (SDs) are shown by error bars.

3.3.2 The culture of pduL2::acetone strain under the H_2-CO_2 condition

It was confirmed that the enzymes related to acetone biosynthesis were functionally expressed in the pduL2::acetone strain under the condition with fructose. When acetone is produced at the maximum efficiency from H_2-CO_2, the net ATP yield is zero, indicating that "ATP shortage" would be a bottleneck in the metabolism in the pduL2::acetone strain:

$$8\ H_2 + 3\ CO_2 \rightarrow \text{Acetone} + 5\ H_2O\ (+\ 0\ \text{ATP})$$

To investigate whether the metabolism would be in "ATP shortage" state, the strain was cultured under the H_2-CO_2 condition. To set up the culture, the strain was inoculated into the basal medium with fructose and was grown until the mid-logarithmic phase. Then, the strain was transferred into the fresh medium with H_2-CO_2 in the headspace of the vial for the pre-culture. This step was performed to completely consume fructose and to adapt the strain to the H_2-CO_2 condition. Finally, the adapted cells were inoculated into the new fresh medium supplemented with H_2-CO_2. There was almost no growth during 254 h of cultivation time (Fig. 3-3A). Excreted metabolites accumulated over time (Fig. 3-3B), indicating that the cells were metabolically active. Acetone was successfully produced under the H_2-CO_2 condition, reaching 1.8 ± 0.08 mM in the culture medium after 254 h. This result indicated that the enzymes of acetone biosynthesis were functionally expressed in the H_2-CO_2 condition. However, acetate production reached 3.3 ± 0.09 mM and was dominant over acetone production. Formate accumulated in the culture medium, reaching 1.2 ± 0.12 mM. Formate is an intermediate compound in the WLP, and ATP is required to convert formate to acetyl-CoA (Fig. 1-2). Therefore, the accumulation of formate indicated that the metabolism was in "ATP shortage" under the H_2-CO_2 condition.

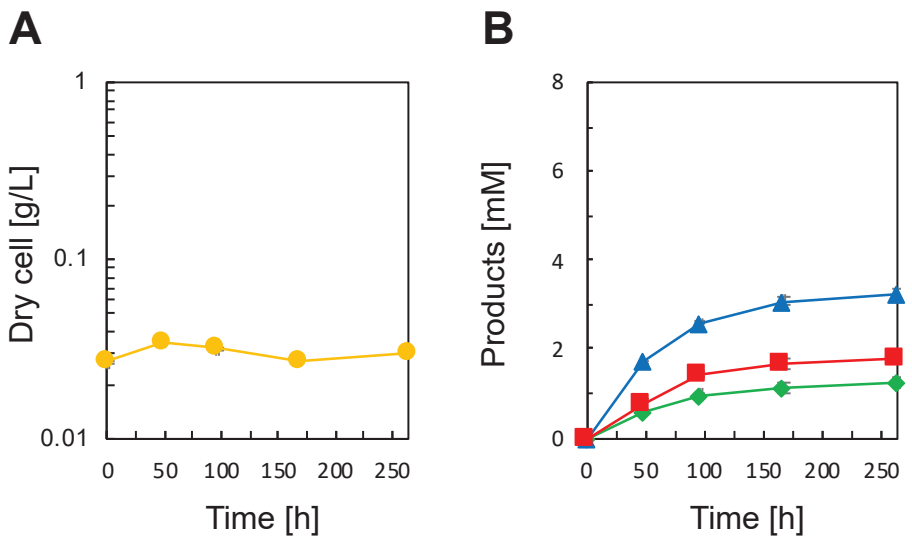

Fig. 3-3 Growth and fermentation products of the pduL2::acetone strain under H_2-CO_2 as the substrate. (**A**) Dry cell weight according to the OD under the H_2-CO_2 condition. (**B**) Concentrations of excreted metabolites under the H_2-CO_2 condition were measured by HPLC. Symbols: ●, Dry cell weight; ■, Acetone; ▲, Acetate; ◆, Formate. The experiment was performed in triplicates, and standard deviations (SDs) are shown by error bars. Most error bars showing a small error range overlapped with symbols of data plots.

3.3.3 The effect of electron acceptors on H_2-dependent growth of pduL2::acetone strain

The purpose of constructing the acetone-producing strain is to separate multiple issues and investigate "ATP shortage". In the H_2-CO_2 condition, the pduL2::acetone strain did not grow and produced formate, indicating that the metabolism is in "ATP shortage" state. Thus, the H_2-CO_2 culture of the pduL2::acetone strain would be the condition that results in an ATP deficient state.

Acetogens employ ion gradient-driven phosphorylation (IGP) by using proton or sodium gradient across the membrane and drive ATP formation by F_0F_1-ATPase [17; 50; 70; 71]. One strategy to overcome the energetic barriers in autotrophic conditions without substrate-level phosphorylation (SLP) would be the enhancement of the level of IGP [31]. In addition to CO_2, it is known that acetogens can reduce several substrates such as pyruvate [72], fumarate [73; 74], aromatic acrylates [75; 76; 77], inorganic sulfur compounds [78; 79; 80], and nitrate or nitrite. [81; 82; 83; 84]. Moreover, the use of these electron acceptors was, in some instances, shown to be coupled to energy conservation in autotrophic conditions on H_2-CO_2 [71; 85]. Under heterotrophic conditions, it was reported that *M. thermoacetica* also can use nitrate, nitrite, dimethyl sulfoxide (DMSO), and thiosulfate as electron acceptors, and energy conservation was enhanced [70; 81; 84]. Therefore, to evaluate the effect of electron acceptors on the H_2-dependent growth of the pduL2::acetone strain, the strain was cultured in the presence of electron acceptors which can be utilized by *M. thermoacetica*. Table 3-3 provides the H_2-CO_2 culture profile with or without electron acceptors. The dry cell weight was increased in the conditions with nitrate, thiosulfate, and DMSO compared to without these electron acceptors, while the weight was decreased in the presence of nitrite. In particular, the weight under the

condition with DMSO was 128.4 ± 4.4 mg/L, which was the highest value among the conditions with electron acceptors. Acetone and acetate productivity was higher with DMSO or thiosulfate than without these electron acceptors, whereas any metabolites were not detected from the medium with nitrate and nitrite. The specific acetone productivity with DMSO or thiosulfate is 0.6 ± 0.0 or 0.2 ± 0.0 mmol/g-cell/h, respectively, indicating that the effect of DMSO on acetone productivity was greater than the condition with thiosulfate. Therefore, it was indicated that the addition of electron acceptors to the H_2-CO_2 condition improves the growth and acetone productivity of the pduL2::acetone strain, and DMSO is the most suitable electron acceptor, especially among the electron acceptors used in this study.

Under standard states and with H_2-derived reductant, the reductive reactions, and the change in the Gibbs free energy for the reduction of each electron acceptor are as follows [84; 86; 87].

Nitrate: $NO_3^- + 4H_2 + 2H^+ \rightarrow NH_4^+ + 3H_2O$ -75 kJ/mol-reducing equivalent

Nitrite: $NO_2^- + 3H_2 + 2H^+ \rightarrow NH_4^+ + 2H_2O$ -73 kJ/mol-reducing equivalent

Dimethyl sulfoxide: $DMSO + H_2 \rightarrow DMS + H_2O$ -55 kJ/mol-reducing equivalent

Thiosulfate: $S_2O_3^{2-} + 4H_2 \rightarrow 2HS^- + 3H_2O$ -22 kJ/mol-reducing equivalent

From these values, nitrate or nitrite reduction is more favorable energetically than DMSO or thiosulfate, which appears to further increase growth and production. However, the addition of DMSO or thiosulfate was more effective for growth and production than nitrate or nitrite, which is inconsistent with the theory. In the wild strain of *M. thermoacetica*, the presence of nitrate or nitrite inhibits acetate generation through the WLP, indicating that the CO_2 metabolism is repressed by nitrate or nitrite [82; 84]. Therefore, the inconsistent results with theory would be caused by blocking the CO_2

metabolism of the pduL2::acetone strain. It is not clear why the addition of nitrate and nitrite inhibits the CO_2 metabolism of *M. thermoaccetica*. One study reported that the activity of the WLP enzymes was not affected by the addition of nitrate, whereas another study reported that the synthesis of the WLP enzymes was downregulated by nitrate supplementation [82; 83]. Some studies reported that the *b*-type cytochrome was not formed in the presence of nitrate or nitrite, but it is not clear whether the cytochrome is involved in the transfer of electrons to and from WLP enzymes [82; 83; 84; 88; 89]. In this study, the results of the addition of DMSO and thiosulfate indicated that the CO_2 metabolism of *M. thermoaccetica* is not blocked by the presence of these electron acceptors. This finding would contribute to an investigation into why nitrate and nitrite inhibit WLP.

Table 3-3. H_2-CO_2 culture profile of pduL2::acetone strain with or without electron acceptors at 168 h of the cultivated time. (Initial conc. of electron acceptors: 50 mM)

Electron acceptor	ΔDry cell[a]	ΔAcetate[a]	ΔAcetone[a]	Specific rate of acetone
	mg/L	mM	mM	mmol/g-cell/h
None	11.1 ± 3.0	1.5 ± 0.5	0.0 ± 0.0	0.0 ± 0.0
DMSO	128.3 ± 4.4	5.3 ± 0.2	4.0 ± 0.2	0.6 ± 0.0
Thiosulfate	47.1 ± 7.4	2.5 ± 0.2	1.8 ± 0.4	0.2 ± 0.0
Nitrate	32.3 ± 0.4	0.0 ± 0.0	0.0 ± 0.0	0.0 ± 0.0
Nitrite	4.2 ± 0.4	0.0 ± 0.0	0.0 ± 0.0	0.0 ± 0.0

[a] The difference in the value was calculated by subtracting the initial value from the maximum value.

3.3.4 Analysis of the change of H_2-CO_2 culture profile by DMSO supplementation.

DMSO supplementation increased growth and acetone production more than other electron acceptors supplementation. To analyze the effect of DMSO supplementation on the H_2-CO_2 culture profile in more detail, the pduL2::acetone strain was again cultured under the H_2-CO_2 condition with or without DMSO. The strain started to consume DMSO just after inoculating into the medium, and it was not detected from 144 h (Fig. 3-4A). Although formate was produced in both conditions, it was detected later with DMSO than without it (Fig. 3-4F). In the condition with DMSO, formate detection and DMSO disappearance were at almost the same time (Fig. 3-4A and F). The presence of DMSO in the medium increased growth, H_2 consumption, and acetate and acetone production (Fig. 3-4B-E). The strain started to grow just after inoculating into the DMSO presence medium and continued to grow until 121 h (Fig. 3-4B). The growth rate with DMSO was 0.017 ± 0.000 [/h]. Acetate was detected in both conditions and the production was similar until 121 h (Fig. 3-4D). After 121 h, the production with DMSO was higher than without DMSO. Acetone was detected only in the condition with DMSO (Fig 3-4E). The production reached 3.4 mM at 168 h. H_2 was consumed by the strain in both conditions with and without DMSO (Fig. 3-4C). H_2 consumption with or without DMSO until 168 h was 2.11 ± 0.03 or 0.70 ± 0.01 mmol, respectively (Table 3-4). The cellular yield for H_2 consumption ($Y_{Cell/H2}$) increased to 1.20 ± 0.05 g/mol with DMSO, from 0.16 ± 0.05 g/mol without DMSO (Table 3-4). Since H_2-dependent growth is ATP-limited, this result implied that additional ATP was generated by DMSO supplementation. To investigate the effect of DMSO on ATP productivity, the intracellular ATP level of the strain was measured (Fig. 3-4G). The level with or without DMSO was 87.7 ± 12.4 or 8.7 ± 3.3 nmol/g-cell, respectively. It was demonstrated that DMSO supplementation enhanced

ATP production, growth, and metabolites production under the H_2-CO_2 culture., showing that “ATP shortage” is a bottleneck in the metabolism in the metabolically engineered strains to be used for gas fermentation. In addition, the supplementation of electron acceptors can be a candidate strategy to overcome the bottleneck.

DMSO is reduced to dimethyl sulfide (DMS) by DMSO reductase [70; 90]. The genome of *M. thermoacetica* harbors genes encoding DMSO reductase, and the enzyme is present in the cell membrane of *M. thermoacetica* [91; 92]. DMSO and DMS are organic compounds containing two methyl groups. It is known that *M. thermoacetica* can utilize the methyl group of several methylated compounds as carbon and energy source. To investigate whether *M. thermoacetica* utilized DMSO and DMS as carbon and energy source, the amount of consumed DMSO and generated DMS was measured at the initial and final culture point (Table 3-4). The DMSO detected at the initial point was completely consumed by the final point (Fig 3-4A). DMS, which was not present at the initial point, was detected by GC-MS analysis at the final point, and the amount reached 0.92 ± 0.02 mmol. The DMS yield per DMSO consumption was 0.90 ± 0.03 mol/mol, indicating that almost all the consumed DMSO was reduced to DMS, and it was not further metabolized (Table 3-4). Therefore, *M. thermoacetica* does not appear to be able to use DMSO and DMS as a carbon and energy source.

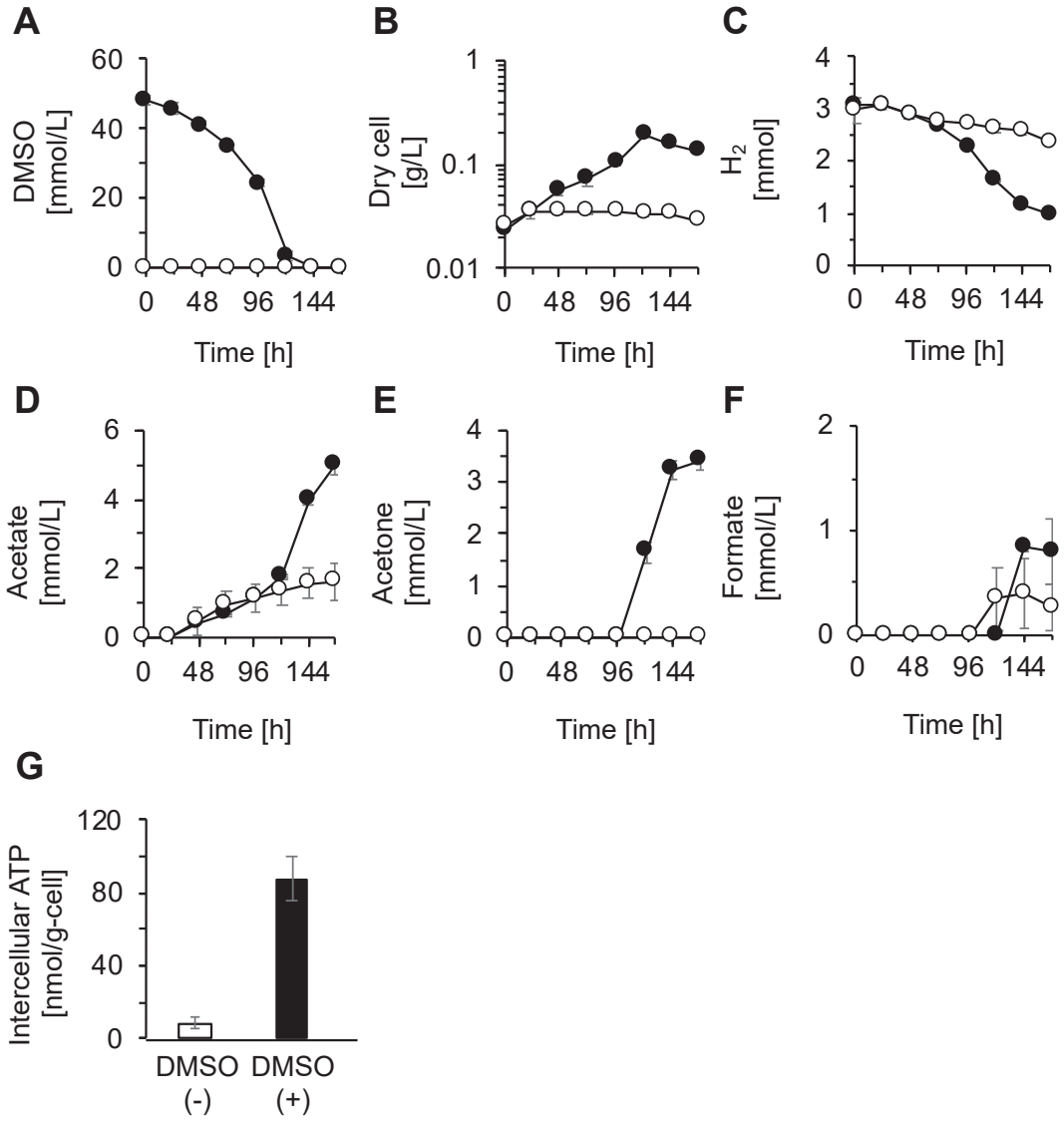

Fig 3-4 Effect of DMSO supplementation on H_2-dependent growth of the pduL2::acetone strain. **(A)** DMSO consumption, **(B)** Dry cell weight according to the optical density, **(C)** H_2 consumption, **(D)** acetate production, **(E)** acetone production, and **(F)** formate production in the presence of DMSO (●) and its absence (○). **(G)** The intracellular ATP level with or without DMSO. The experiment was performed in triplicates, and standard deviations (SDs) are shown by error bars. Most error bars showing a small error range overlapped with symbols of data plots. All cultures were provided with the same amount of H_2 and CO_2.

Table 3-4. Effect of DMSO on cell formation and the fate of DMSO

Substrate	Cell formation			DMSO reduction		
	ΔDry cell[a]	ΔH_2[a]	Cell/H_2	ΔDMSO[a]	ΔDMS[a]	DMS/DMSO
	mg/L	mmol	g/mol	mmol	mmol	mol/mol
H_2	0.11 ± 0.03	0.70 ± 0.01	0.16 ± 0.05	-	-	-
H_2 + DMSO	2.53 ± 0.10	2.11 ± 0.03	1.20 ± 0.05	1.02 ± 0.03	0.92 ± 0.02	0.90 ± 0.03

[a] The difference in the value was calculated by subtracting the initial value from the maximum value.

3.3.5 CO provides sufficient ATP for autotrophic growth using no electron acceptors.

It was shown that "ATP shortage" is a bottleneck in the metabolism in metabolically engineered strains to be used for gas fermentation. CO is a more ATP-productive gas substrate than H_2 (Fig 1-3). When using the CO-containing gases, acetone is produced as follows:

$$8\ CO + 3\ H_2O \rightarrow Acetone + 5\ CO_2\ (+\ 2\ ATP)$$

$$3\ CO + 5\ H_2 \rightarrow Acetone + 2\ H_2O\ (+\ 0.75\ ATP)$$

In theory, when CO is metabolized by *M. thermoacetica*, net ATP yield is positive even if acetone is produced at maximum yield, indicating that the supplement of electron acceptors is not necessary to provide sufficient ATP for autotrophic growth. To test whether growth and producing acetone in the presence of CO, the pduL2::acetone strain was cultured in the CO-containing conditions (CO-CO_2 and CO-H_2-CO_2) without the use of electron acceptors. To adapt the strains to the condition, the strains were cultured with a similar method when the strains were adapted to H_2-CO_2. The gas composition was changed to CO-CO_2 or CO-H_2-CO_2 from H_2-CO_2. First, the strain was cultured in the CO-CO_2 condition and cell biomass was increased, indicating that sufficient ATP was supplied for autotrophic growth without the no electron acceptors (Fig. 3-5A). Acetone was produced in addition to acetate (Fig. 3-5C). The acetone-acetate ratio was 0.27 ± 0.01 mol-acetone/mol-acetate, indicating that acetate is dominant compared to acetone. Next, the strain was cultured in the CO-H_2-CO_2 condition (Fig. 3-5B and D). Whereas the culture profile showed almost the same cell biomass and growth rate as in the CO-CO_2 condition, the acetone titer significantly improved from 1.1 ± 0.04 to 3.3 ± 0.1 mM and the increment was higher compared to acetate (from 4.2 ± 0.08 to 7.0 ± 0.10 mM). These results indicate that carbon flux to the acetone biosynthesis pathway was enhanced by the

addition of H_2. The acetone-acetate ratio increased from 0.27 ± 0.01 to 0.47 ± 0.01 mol-acetone/mol-acetate and was still acetate dominant, but was higher than the CO-CO_2 condition. Moreover, the maximum specific acetone production rate also increased from 0.04 ± 0.00 to 0.09 ± 0.01 g-acetone /g-dry cell/ h by adding H_2.

The growth and metabolite profiles of the autotrophic acetone production in both CO-containing conditions can be compared by the fermentation parameters summarized in Table 3-5. Since H_2 supplementation did not affect cell growth, it appears that the electrons derived from H_2 were invested in acetone and acetate production rather than cellular biomass. It was also indicated that the electron input was directed to acetone rather than acetate.

The pduL2::acetone strain produced acetone and grew under the CO-CO_2 conditions, and the acetone production was enhanced by H_2 supplementation. The theoretical acetone yield for the consumed CO with and without H_2 is 0.33 and 0.13 mol-acetone/mol-CO, respectively. In theory, acetone production should be higher due to the addition of H_2. The consumption of CO was similar in both conditions and H_2 was consumed in the presence of H_2 (Table 3-5). In our experiment with the pduL2::acetone strain, H_2 addition significantly improved acetone production to higher compared to the CO-CO_2 condition (Fig. 3-5C and D, Table 3-5). On the other hand, acetate was detected in both conditions, indicating that acetyl-CoA was not efficiently converted to acetone. In the above formulas, the net ATP yield is positive in both conditions, meaning that the net acetate production is not required for maintaining autotrophic growth and producing acetone. Thus, if the final amount of acetate turns to zero and the flow of acetyl-CoA is optimized, acetone production could be improved in both gaseous conditions. One explanation for the accumulation of acetate may be the limitation of the enzymatic

reaction, such as the CoA transferase that transfers CoA from acetoacetyl-CoA to acetate (Fig 3-1A). It is reported that the enzyme requires a high acetate concentration to start solventogenesis in *C. acetobutylicum* because CoA transferase shows a high K_m of 1200 mM against acetate [93]. Although the enzymatic properties of CoA transferase were not analyzed in this study, it is conceivable that the enzyme has a high K_m against acetate and that the acetate concentration is a limiting factor. In fact, a higher concentration of acetate was obtained in the culture with fructose (Fig. 3-2D). Therefore, it would be required for enhancing acetone productivity to utilize protein engineering such as improving the K_m against acetate and increasing the V_{max} of selected enzymes. In addition, it may also be desirable to inhibit the expression of the PduL1, which is responsible for supplying acetate in the pduL2::acetone strain, or replace the enzyme itself with its homolog with the large K_m value.

Table 3-5 Fermentation parameters for acetone production from CO-containing gas.

Substrate	Consumed substrates		Yield for CO				Recovery		Specific rate of acetone
	CO	H_2	Cell biomass	Acetate	Acetone	CO_2	Carbon	Electron	
	mmol	mmol	g/mol	mol/mol	mol/mol	mol/mol	%	%	g/g-cell/h
CO-CO_2	1.18 ± 0.03	N.A.[a]	2.04 ± 0.03	0.155 ± 0.00	0.041 ± 0.00	0.487 ± 0.016	101.1 ± 1.4	115.4 ± 2.5	0.04 ± 0.00
CO-H_2-CO_2	1.18 ± 0.04	1.10 ± 0.05	2.01 ± 0.03	0.251 ± 0.01	0.117 ± 0.00	0.277 ± 0.041	119.6 ± 2.4	110.2 ± 1.9	0.09 ± 0.00

[a] Not applied

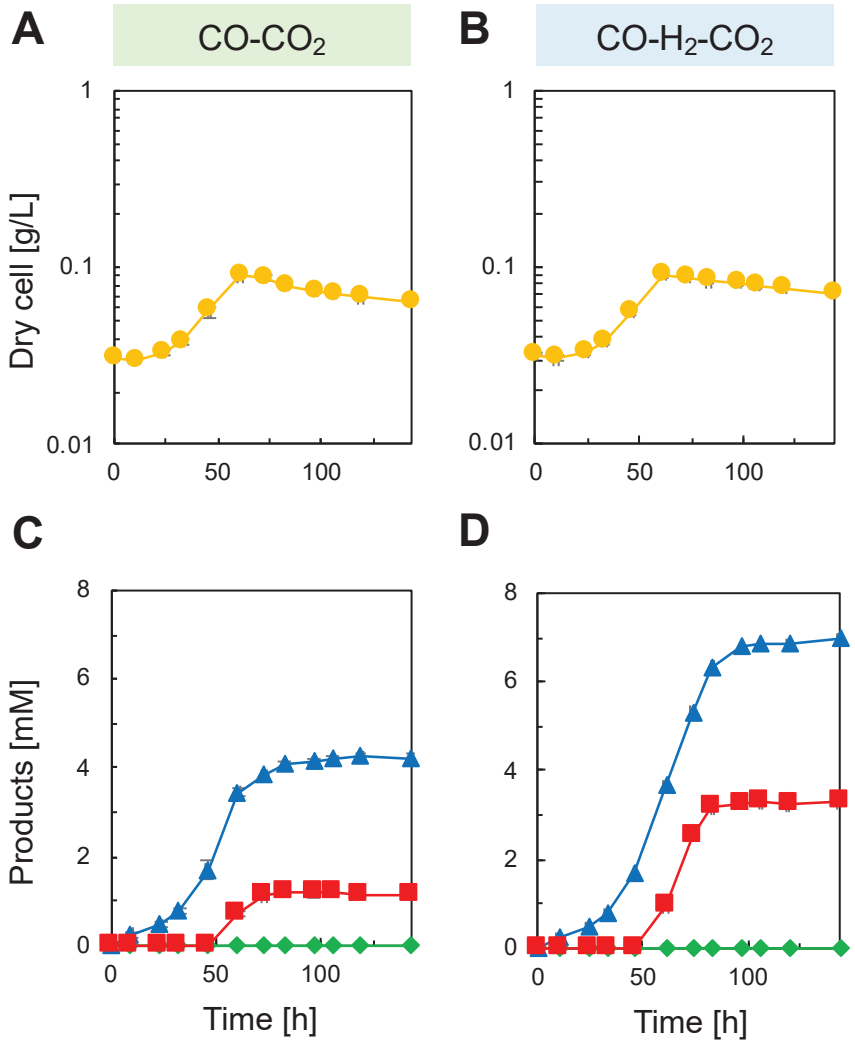

Fig. 3-5 Growth and fermentation products of the pduL2::acetone strain under CO-CO_2 and CO-H_2-CO_2. (**A**) Dry cell weight according to the OD under the CO-CO_2 condition. (**B**) Concentrations of excreted metabolites under the CO-CO_2 condition were measured by HPLC. (**C**) Dry cell weight according to the OD under the CO-H_2-CO_2 condition. (**D**) Excreted metabolites under the CO-H_2-CO_2 condition were measured by HPLC. Symbols: ●, Dry cell weight; ■, Acetone; ▲, Acetate; ◆, Formate. The experiment was performed in triplicates, and standard deviations (SDs) are shown by error bars. Most error bars showing a small error range overlapped with symbols of data plots.

3.4 Conclusion

In this chapter, to separate two bottlenecks and investigate “ATP shortage”, the acetone biosynthesis pathway was introduced into *M. thermoacetica*, and it was found that “ATP shortage” is the bottleneck in the metabolism of metabolically engineered strain to be used for gas fermentation. Since the pathway from acetyl-CoA does not require redox reactions, the redox balance would be maintained as in the acetate production of wild type. Firstly, to test whether the pathway is functional in *M. thermoacetica*, two metabolically engineered strains were cultured under the condition using fructose. Acetone was produced by the strains, indicating that the pathway is functional in both strains. Next, the pduL2::acetone strain, which has higher acetone productivity, was cultured in the H_2-CO_2 condition and successfully produced acetone. In addition, the strain did not grow, and formate was accumulated in the medium, indicating that the metabolism was in “ATP shortage” state. To supply ATP, several electron acceptors were added to the H_2-CO_2 condition, resulting in the growth recovery and increased acetone production of the pduL2::acetone strain. In fact, the ATP level was significantly enhanced upon DMSO addition. These results showed that “ATP shortage” is a bottleneck in the metabolism of metabolically engineered strains to be used for gas fermentation. In the conditions using CO, it is not necessary that electron acceptors are added to provide sufficient ATP for autotrophic growth. Therefore, to enhance the performance of metabolically engineered strains used for gas fermentation, it is important that the metabolic pathway is designed to avoid “redox imbalance” and maintain the sufficient level of ATP. The supplementation of electron acceptors may be a candidate strategy to enhance ATP production.

Chapter 4

Chapter 4. Concluding remarks

This thesis described the successful development of a technology to produce important chemicals from gaseous substrates using metabolically engineered *M. thermoacetica*, a thermophilic acetogen. In chapter 2, the Mt-Δ*pduL2*::*aldh* strain produced ethanol from CO-containing gaseous substrates. In chapter 3, the pduL2::acetone strain produced acetone from several gaseous substrates. The gas fermentation processes using thermophilic acetogens have several benefits compared to mesophiles. Furthermore, one potential application is simplified and cost-effective gas fermentation systems that can simultaneously collect volatile chemicals by distillation during fermentation. Since *M. thermoacetica* grows at temperatures near the boiling point of ethanol or acetone, it is possible to build and evaluate such gas fermentation systems. In particular, the boiling point of acetone (56 °C) is lower than the growth temperature of *M. thermoacetica* (45-65 °C), and acetone would be a more suitable chemical than ethanol for evaluating the gas fermentation systems with simultaneous distillation.

Moreover, in this thesis, it was indicated that there are multiple bottlenecks in the metabolism of metabolically engineered stains to be used for gas fermentation. In chapter 2, almost no ATP was detected in the ethanol-producing strains cultured under the H_2-CO_2 condition, indicating that the metabolism was in "ATP shortage" state. Under the CO-CO_2 condition, although ATP levels were high, the available NADH of the Mt-Δ*pduL1*Δ*pduL2*::*aldh* strain was significantly lower than that of the Mt-Δ*pduL2*::*aldh* strain, and this poor NADH level was consistent with the result of no ethanol production. These results indicated that the redox state was unbalanced. Therefore, it was indicated that "ATP shortage" and "redox imbalance" are bottlenecks in the metabolism of

metabolically engineered stains for gas fermentation. In chapter 3, to separate the two bottlenecks and investigate “ATP shortage” as the only bottleneck, the pduL2::acetone strain was constructed. Since the acetone biosynthesis pathway from acetyl-CoA does not require redox reactions, the redox balance would be maintained as in the acetate production of wild type. In the H_2-CO_2 condition, the strain did not grow, and formate was detected, indicating that the metabolism was in “ATP shortage” state. To supply ATP, several electron acceptors including DMSO were added to the culture, resulting in the growth recovery and increased acetone production of the pduL2::acetone strain. In fact, ATP level was significantly enhanced upon DMSO supplementation. These results showed that “ATP shortage” is the only bottleneck in the metabolism of metabolically engineered stains, in which the redox balance is maintained. Therefore, to enhance gas fermentation by metabolically engineered strains, it is important that the metabolic pathway is designed to avoid “redox imbalance” and maintain the sufficient level of ATP.

In chapter 3, it was shown that ATP production was enhanced by the addition of DMSO. However, it is an expensive chemical (¥38000 kg^{-1}; anhydrous, ≧99.0 %; Sigma-Aldrich) and its use would raise the market price of the products by gas fermentation. Therefore, it will be necessary to search for cheaper alternatives. Nitrate is a cheaper electron acceptor than DMSO and nitrate reduction is more energetically favorable than DMSO. On the other hand, nitrate blocks the autotrophic growth of *M. thermoacetica*. Thus, it will be necessary to construct a strain that is capable of autotrophic growth even in the presence of nitrate. The findings with DMSO may help to provide some insights into the design of such strain.

As such, I believe this thesis provided important results and insights that contribute to the development of gas fermentation, especially with thermophilic bacteria.

Reference

[1] L. Wei, L.O. Pordesimo, C. Igathinathane, and W.D. Batchelor, Process engineering evaluation of ethanol production from wood through bioprocessing and chemical catalysis. Biomass and Bioenergy 33 (2009) 255-266.

[2] S.N. Naik, V.V. Goud, P.K. Rout, and A.K. Dalai, Production of first and second generation biofuels: A comprehensive review. Renewable and Sustainable Energy Reviews 14 (2010) 578-597.

[3] C.C. Geddes, I.U. Nieves, and L.O. Ingram, Advances in ethanol production. Curr Opin Biotechnol 22 (2011) 312-9.

[4] T.R. Brown, and R.C. Brown, A review of cellulosic biofuel commercial-scale projects in the United States. Biofuels, Bioproducts and Biorefining 7 (2013) 235-245.

[5] S. Haghighi Mood, A. Hossein Golfeshan, M. Tabatabaei, G. Salehi Jouzani, G.H. Najafi, M. Gholami, and M. Ardjmand, Lignocellulosic biomass to bioethanol, a comprehensive review with a focus on pretreatment. Renewable and Sustainable Energy Reviews 27 (2013) 77-93.

[6] Y. Sun, and J. Cheng, Hydrolysis of lignocellulosic materials for ethanol production: a review. Bioresour Technol 83 (2002) 1-11.

[7] H.N. Abubackar, M.C. Veiga, and C. Kennes, Biological conversion of carbon monoxide: rich syngas or waste gases to bioethanol. Biofuels, Bioproducts and Biorefining 5 (2011) 93-114.

[8] J. Daniell, M. Köpke, and S. Simpson, Commercial Biomass Syngas Fermentation. Energies 5 (2012) 5372-5417.

[9] F. Liew, M.E. Martin, R.C. Tappel, B.D. Heijstra, C. Mihalcea, and M. Kopke, Gas Fermentation-A Flexible Platform for Commercial Scale Production of Low-

Carbon-Fuels and Chemicals from Waste and Renewable Feedstocks. Front Microbiol 7 (2016) 694.

[10] B. Molitor, H. Richter, M.E. Martin, R.O. Jensen, A. Juminaga, C. Mihalcea, and L.T. Angenent, Carbon recovery by fermentation of CO-rich off gases - Turning steel mills into biorefineries. Bioresour Technol 215 (2016) 386-396.

[11] M. Köpke, and S.D. Simpson, Pollution to products: recycling of 'above ground' carbon by gas fermentation. Curr Opin Biotechnol 65 (2020) 180-189.

[12] R.K. Thauer, Microbiology. A fifth pathway of carbon fixation. Science 318 (2007) 1732-3.

[13] A.G. Fast, and E.T. Papoutsakis, Stoichiometric and energetic analyses of non-photosynthetic CO_2-fixation pathways to support synthetic biology strategies for production of fuels and chemicals. Current Opinion in Chemical Engineering 1 (2012) 380-395.

[14] H.G. Wood, Life with CO or CO_2 and H_2 as a source of carbon and energy. Faseb j 5 (1991) 156-63.

[15] S.W. Ragsdale, and E. Pierce, Acetogenesis and the Wood-Ljungdahl pathway of CO(2) fixation. Biochim Biophys Acta 1784 (2008) 1873-98.

[16] H. Latif, A.A. Zeidan, A.T. Nielsen, and K. Zengler, Trash to treasure: production of biofuels and commodity chemicals via syngas fermenting microorganisms. Curr Opin Biotechnol 27 (2014) 79-87.

[17] K. Schuchmann, and V. Muller, Autotrophy at the thermodynamic limit of life: a model for energy conservation in acetogenic bacteria. Nat Rev Microbiol 12 (2014) 809-21.

[18] B.R. Sharak Genthner, and M.P. Bryant, Additional characteristics of one-carbon-

compound utilization by *Eubacterium limosum* and *Acetobacterium woodii*. Appl Environ Microbiol 53 (1987) 471-6.

[19] A.D. Adamse, New isolation of *Clostridium aceticum* (Wieringa). Antonie Van Leeuwenhoek 46 (1980) 523-31.

[20] M. Braun, F. Mayer, and G. Gottschalk, *Clostridium aceticum* (Wieringa), a microorganism producing acetic acid from molecular hydrogen and carbon dioxide. Arch Microbiol 128 (1981) 288-93.

[21] J. Abrini, H. Naveau, and E.J. Nyns, *Clostridium autoethanogenum*, sp. nov., an anaerobic bacterium that produces ethanol from carbon monoxide. Archives of Microbiology 161 (1994) 345-351.

[22] M. Köpke, C. Mihalcea, F. Liew, J.H. Tizard, M.S. Ali, J.J. Conolly, B. Al-Sinawi, and S.D. Simpson, 2,3-butanediol production by acetogenic bacteria, an alternative route to chemical synthesis, using industrial waste gas. Appl Environ Microbiol 77 (2011) 5467-75.

[23] R.S. Tanner, L.M. Miller, and D. Yang, *Clostridium ljungdahlii* sp. nov., an acetogenic species in clostridial rRNA homology group I. Int J Syst Bacteriol 43 (1993) 232-6.

[24] M. Köpke, C. Held, S. Hujer, H. Liesegang, A. Wiezer, A. Wollherr, A. Ehrenreich, W. Liebl, G. Gottschalk, and P. Dürre, *Clostridium ljungdahlii* represents a microbial production platform based on syngas. Proc Natl Acad Sci U S A 107 (2010) 13087-92.

[25] R. Kerby, and J.G. Zeikus, Growth of *Clostridium thermoaceticum* on H_2/CO_2 or CO as energy source. Current Microbiol 8 (1983) 27-30.

[26] S.L. Daniel, T. Hsu, S.I. Dean, and H.L. Drake, Characterization of the H_2- and CO-

dependent chemolithotrophic potentials of the acetogens *Clostridium thermoaceticum* and *Acetogenium kivui*. J Bacteriol 172 (1990) 4464-71.

[27] M.D. Savage, and H.L. Drake, Adaptation of the acetogen *Clostridium thermoautotrophicum* to minimal medium. J Bacteriol 165 (1986) 315-8.

[28] L. J.A., M. F., and W. R.S., Acetogenium kivui, a new thermophilic hydrogen-oxidizing, acetogenic bacterium. Archives of Microbiology 129 (1981) 275-280.

[29] L.J. A., and W.R. S., Acetogenium kivui gen. nov., sp. nov., a thermophilic acetogenic bacterium. INTERNATIONAL JORNAL OF SYSTEMATIC BACTERIOLOGY 33 (1983) 886.

[30] M.C. Weghoff, and V. Müller, CO Metabolism in the Thermophilic Acetogen *Thermoanaerobacter kivui*. Appl Environ Microbiol 82 (2016) 2312-2319.

[31] A. Katsyv, and V. Müller, Overcoming Energetic Barriers in Acetogenic C1 Conversion. Front Bioeng Biotechnol 8 (2020) 621166.

[32] S. Sakai, Y. Nakashimada, K. Inokuma, M. Kita, H. Okada, and N. Nishio, Acetate and ethanol production from H_2 and CO_2 by *Moorella* sp. using a repeated batch culture. J Biosci Bioeng 99 (2005) 252-8.

[33] A. Kita, Y. Iwasaki, S. Sakai, S. Okuto, K. Takaoka, T. Suzuki, S. Yano, S. Sawayama, T. Tajima, J. Kato, N. Nishio, K. Murakami, and Y. Nakashimada, Development of genetic transformation and heterologous expression system in carboxydotrophic thermophilic acetogen *Moorella thermoacetica*. J Biosci Bioeng 115 (2013) 347-52.

[34] M. Basen, I. Geiger, L. Henke, and V. Müller, A Genetic System for the Thermophilic Acetogenic Bacterium *Thermoanaerobacter kivui*. Appl Environ Microbiol 84 (2018).

[35] F. Rahayu, Y. Kawai, Y. Iwasaki, K. Yoshida, A. Kita, T. Tajima, J. Kato, K. Murakami, T. Hoshino, and Y. Nakashimada, Thermophilic ethanol fermentation from lignocellulose hydrolysate by genetically engineered *Moorella thermoacetica*. Bioresour Technol 245 (2017) 1393-1399.

[36] Y. Iwasaki, A. Kita, K. Yoshida, T. Tajima, S. Yano, T. Shou, M. Saito, J. Kato, K. Murakami, and Y. Nakashimada, Homolactic Acid Fermentation by the Genetically Engineered Thermophilic Homoacetogen *Moorella thermoacetica* ATCC 39073. Appl Environ Microbiol 83 (2017).

[37] S. Hoffmeister, M. Gerdom, F.R. Bengelsdorf, S. Linder, S. Flüchter, H. Öztürk, W. Blümke, A. May, R.J. Fischer, H. Bahl, and P. Dürre, Acetone production with metabolically engineered strains of *Acetobacterium woodii*. Metab Eng 36 (2016) 37-47.

[38] B. Schiel-Bengelsdorf, and P. Dürre, Pathway engineering and synthetic biology using acetogens. FEBS Lett 586 (2012) 2191-8.

[39] A.P. Mueller, M. Koepke, and S. Nagaraju, Recombinant Microorganisms and Uses Therefor. in: D.U.S.P.a.T.O. Washington, (Ed.), US 20130330809 A1, LanzaTech New Zealand Limited, United state, 2013.

[40] M. Köpke, S. Simpson, F.M. Liew, and W. Chen, Fermentation Process for Producing Isopropanol Using a Recombinant Microorganism. in: D.U.S.P.a.T.O. Washington, (Ed.), US 9365868 B2, United States 2016.

[41] F.E. Liew, R. Nogle, T. Abdalla, B.J. Rasor, C. Canter, R.O. Jensen, L. Wang, J. Strutz, P. Chirania, S. De Tissera, A.P. Mueller, Z. Ruan, A. Gao, L. Tran, N.L. Engle, J.C. Bromley, J. Daniell, R. Conrado, T.J. Tschaplinski, R.J. Giannone, R.L. Hettich, A.S. Karim, S.D. Simpson, S.D. Brown, C. Leang, M.C. Jewett, and M.

Köpke, Carbon-negative production of acetone and isopropanol by gas fermentation at industrial pilot scale. Nature Biotechnology (2022).

[42] M. Köpke, and W.Y. Chen, Recombinant Microorganisms and Uses Therefor. in: D.U.S.P.a.T.O. Washington, (Ed.), US 2013/0323806 A1, LanzaTech New Zealand Limited, United States, 2013.

[43] F. Liew, and M. Köpke, Recombinant Microorganisms Make Biodiesel. in: D.U.S.P.a.T.O. Washington, (Ed.), US 9347076 B2, LANZATECH NEW ZEALAND LIMITED, United States, 2016.

[44] W. Chen, F. Liew, and M. Koepke, Recombinant Microorganisms and Uses Therefor. in: D.U.S.P.a.T.O. Washington, (Ed.), US 2013/0323820 A1, LanzaTech New Zealand Limited, United States, 2013.

[45] A. Banerjee, C. Leang, T. Ueki, K.P. Nevin, and D.R. Lovley, Lactose-inducible system for metabolic engineering of *Clostridium ljungdahlii*. Appl Environ Microbiol 80 (2014) 2410-6.

[46] T. Ueki, K.P. Nevin, T.L. Woodard, and D.R. Lovley, Converting carbon dioxide to butyrate with an engineered strain of *Clostridium ljungdahlii*. mBio 5 (2014) e01636-14.

[47] B.A. Diner, J. Fan, M.C. Scotcher, D.H. Wells, and G.M. Whited, Synthesis of Heterologous Mevalonic Acid Pathway Enzymes in *Clostridium ljungdahlii* for the Conversion of Fructose and of Syngas to Mevalonate and Isoprene. Appl Environ Microbiol 84 (2018).

[48] D. Jia, M. He, Y. Tian, S. Shen, X. Zhu, Y. Wang, Y. Zhuang, W. Jiang, and Y. Gu, Metabolic Engineering of Gas-Fermenting *Clostridium ljungdahlii* for Efficient Co-production of Isopropanol, 3-Hydroxybutyrate, and Ethanol. ACS Synth Biol

10 (2021) 2628-2638.

[49] M.P. Taylor, K.L. Eley, S. Martin, M.I. Tuffin, S.G. Burton, and D.A. Cowan, Thermophilic ethanologenesis: future prospects for second-generation bioethanol production. Trends Biotechnol 27 (2009) 398-405.

[50] M. Basen, and V. Müller, "Hot" acetogenesis. Extremophiles 21 (2017) 15-26.

[51] H. Wen, H. Chen, D. Cai, P. Gong, T. Zhang, Z. Wu, H. Gao, Z. Li, P. Qin, and T. Tan, Integrated in situ gas stripping-salting-out process for high-titer acetone-butanol-ethanol production from sweet sorghum bagasse. Biotechnol Biofuels 11 (2018) 134.

[52] Y. Iwasaki, A. Kita, K. Yoshida, T. Tajima, S. Yano, T. Shou, M. Saito, J. Kato, K. Murakami, and Y. Nakashimada, Homolactic Acid Fermentation by the Genetically Engineered Thermophilic Homoacetogen *Moorella thermoacetica* ATCC 39073. Appl. Environ. Microbiol. 83 (2017) 1-13.

[53] R. Breitkopf, R. Uhlig, T. Drenckhan, and R.J. Fischer, Two propanediol utilization-like proteins of *Moorella thermoacetica* with phosphotransacetylase activity. Extremophiles 20 (2016) 653-61.

[54] R.S. Tanner, L.M. Miller, and D. Yang, *Clostridium ljungdahlii* sp. nov., an Acetogenic Species in Clostridial rRNA Homology Group I. International Journal of Systematic Bacteriology 43 (1993) 232-236.

[55] R.S. Tanner, Monitoring sulfate-reducing bacteria: comparison of enumeration media. Journal of Microbiological Methods, 10(2) (1989) 83-90.

[56] R.S. Tanner, Monitoring sulfate-reducing bacteria: comparison of enumeration media. Journal of Microbiological Methods 10 (1989) 83-90.

[57] T. Miura, A. Kita, Y. Okamura, T. Aki, Y. Matsumura, T. Tajima, J. Kato, and Y.

Nakashimada, Evaluation of marine sediments as microbial sources for methane production from brown algae under high salinity. 169 (2014) 362-366.

[58] T. Miura, A. Kita, Y. Okamura, T. Aki, Y. Matsumura, T. Tajima, J. Kato, and Y. Nakashimada, Evaluation of marine sediments as microbial sources for methane production from brown algae under high salinity. Bioresour Technol 169 (2014) 362-366.

[59] K. Inokuma, Y. Nakashimada, T. Akahoshi, and N. Nishio, Characterization of enzymes involved in the ethanol production of *Moorella* sp. HUC22-1. Arch. Microbiol. 188 (2007) 37-45.

[60] K. Valgepea, R. de Souza Pinto Lemgruber, T. Abdalla, S. Binos, N. Takemori, A. Takemori, Y. Tanaka, R. Tappel, M. Kopke, S.D. Simpson, L.K. Nielsen, and E. Marcellin, H_2 drives metabolic rearrangements in gas-fermenting *Clostridium autoethanogenum*. Biotechnol Biofuels 11 (2018) 55.

[61] J. Mock, Y. Zheng, A.P. Mueller, S. Ly, L. Tran, S. Segovia, S. Nagaraju, M. Kopke, P. Durre, and R.K. Thauer, Energy Conservation Associated with Ethanol Formation from H_2 and CO_2 in *Clostridium autoethanogenum* Involving Electron Bifurcation. J. Bacteriol. 197 (2015) 2965-80.

[62] P. Anbarasan, Z.C. Baer, S. Sreekumar, E. Gross, J.B. Binder, H.W. Blanch, D.S. Clark, and F.D. Toste, Integration of chemical catalysis with extractive fermentation to produce fuels. Nature 491 (2012) 235-9.

[63] A. Rahman, and S. S-Al-Deyab, A review on reduction of acetone to isopropanol with Ni nano superactive, heterogeneous catalysts as an environmentally benevolent approach. Applied Catalysis A: General 469 (2014) 517-523.

[64] C.F. Ryan, C.M. Moore, J.H. Leal, T.A. Semelsberger, J.K. Banh, J. Zhu, C.S.

McEnally, L.D. Pfefferle, and A.D. Sutton, Synthesis of aviation fuel from bio-derived isophorone. Sustainable Energy & Fuels 4 (2020) 1088-1092.

[65] R.J. Schmidt, Industrial catalytic processes—phenol production. Applied Catalysis A: General 280 (2005) 89-103.

[66] D. PM, Bioprocess Engineering Principles. Academic Press (1995) 190-217.

[67] A. Schäfer, A. Tauch, W. Jäger, J. Kalinowski, G. Thierbach, and A. Pühler, Small mobilizable multi-purpose cloning vectors derived from the *Escherichia coli* plasmids pK18 and pK19: selection of defined deletions in the chromosome of Corynebacterium glutamicum. Gene 145 (1994) 69-73.

[68] B.M. Zeldes, C.T. Straub, J.K. Otten, M.W.W. Adams, and R.M. Kelly, A synthetic enzymatic pathway for extremely thermophilic acetone production based on the unexpectedly thermostable acetoacetate decarboxylase from *Clostridium acetobutylicum*. Biotechnol Bioeng 115 (2018) 2951-2961.

[69] A.J. Loder, B.M. Zeldes, G.D. Garrison, 2nd, G.L. Lipscomb, M.W. Adams, and R.M. Kelly, Alcohol Selectivity in a Synthetic Thermophilic n-Butanol Pathway Is Driven by Biocatalytic and Thermostability Characteristics of Constituent Enzymes. Appl Environ Microbiol 81 (2015) 7187-200.

[70] H.L. Drake, and S.L. Daniel, Physiology of the thermophilic acetogen *Moorella thermoacetica*. Res Microbiol 155 (2004) 869-83.

[71] M.C. Schoelmerich, and V. Muller, Energy conservation by a hydrogenase-dependent chemiosmotic mechanism in an ancient metabolic pathway. Proc Natl Acad Sci U S A 116 (2019) 6329-6334.

[72] M. Misoph, and H.L. Drake, Effect of CO_2 on the fermentation capacities of the acetogen Peptostreptococcus productus U-1. J Bacteriol 178 (1996) 3140-5.

[73] M. Dorn, J.R. Andreesen, and G. Gottschalk, Fermentation of fumarate and L-malate by *Clostridium formicoaceticum*. J Bacteriol 133 (1978) 26-32.

[74] C. Matthies, A. Freiberger, and H.L. Drake, Fumarate dissimilation and differential reductant flow by *Clostridium formicoaceticum* and *Clostridium aceticum*. Arch. Microbiol. 160 (1993) 273-278.

[75] R. Bache, and N. Pfernnig, Selective isolation of *Acetobacterium woodii* on methoxylated aromatic acids and determination of growth yields. Arch. Microbiol. 130 (1981) 255-261.

[76] A. Tschech, and N. Pfennig, Growth yield increase linked to caffeate reduction in *Acetobacterium woodii*. Arch Microbiol 137 (1984) 163-167.

[77] M. Misoph, S.L. Daniel, and H.L. Drake, Bidirectional usage of ferulate by the acetogen Peptostreptococcus productus U-1: CO_2 and aromatic acrylate groups as competing electron acceptors. Microbiology 142 (1996) 1983-1988.

[78] P. Beaty, and L. Ljungdahl, Thiosulfate reduction by *Clostridium thermoaceticum* and *Clostridium thermoautotrophicum* during growth, General Meeting of the American Society for Microbiology, 1990.

[79] P. Beaty, and L. Ljungdahl, Growth of *Clostridium thermoaceticum* on methanol, ethanol or dimethylsulfoxide, abstr. K-131, Abstr. 91st Annu. Meet. Am. Soc. Microbiol, 1991, pp. 236.

[80] S. Hattori, Y. Kamagata, S. Hanada, and H. Shoun, Thermacetogenium phaeum gen. nov., sp. nov., a strictly anaerobic, thermophilic, syntrophic acetate-oxidizing bacterium. Int. J. Syst. Evol. Microbiol. 50 (2000) 92-104.

[81] C. Seifritz, S.L. Daniel, A. Gössner, and H.L. Drake, Nitrate as a preferred electron sink for the acetogen *Clostridium thermoaceticum*. J Bacteriol 175 (1993) 8008-

13.

[82] J.M. Fröstl, C. Seifritz, and H.L. Drake, Effect of nitrate on the autotrophic metabolism of the acetogens *Clostridium thermoautotrophicum* and *Clostridium thermoaceticum*. J Bacteriol 178 (1996) 4597-603.

[83] A.F. Arendsen, M.Q. Soliman, and S.W. Ragsdale, Nitrate-dependent regulation of acetate biosynthesis and nitrate respiration by *Clostridium thermoaceticum*. J Bacteriol 181 (1999) 1489-95.

[84] C. Seifritz, H.L. Drake, and S.L. Daniel, Nitrite as an energy-conserving electron sink for the acetogenic bacterium *Moorella thermoacetica*. Curr Microbiol 46 (2003) 329-33.

[85] V. Hess, J.M. Gonzalez, A. Parthasarathy, W. Buckel, and V. Muller, Caffeate respiration in the acetogenic bacterium *Acetobacterium woodii*: a coenzyme A loop saves energy for caffeate activation. Appl Environ Microbiol 79 (2013) 1942-7.

[86] R.K. Thauer, K. Jungermann, and K. Decker, Energy conservation in chemotrophic anaerobic bacteria. Bacteriol Rev 41 (1977) 100-80.

[87] K.H. Nealson, and C.R. Myers, Microbial reduction of manganese and iron: new approaches to carbon cycling. Appl Environ Microbiol 58 (1992) 439-43.

[88] J. Mock, S. Wang, H. Huang, J. Kahnt, and R.K. Thauer, Evidence for a hexaheteromeric methylenetetrahydrofolate reductase in *Moorella thermoacetica*. J Bacteriol 196 (2014) 3303-14.

[89] F.P. Rosenbaum, and V. Müller, Energy conservation under extreme energy limitation: the role of cytochromes and quinones in acetogenic bacteria. Extremophiles 25 (2021) 413-424.

[90] R.J. Turner, J.L. Busaan, J.H. Lee, M. Michalak, and J.H. Weiner, Expression and epitope tagging of the membrane anchor subunit (DmsC) of *Escherichia coli* dimethyl sulfoxide reductase. Protein Eng 10 (1997) 285-90.

[91] E. Pierce, G. Xie, R.D. Barabote, E. Saunders, C.S. Han, J.C. Detter, P. Richardson, T.S. Brettin, A. Das, L.G. Ljungdahl, and S.W. Ragsdale, The complete genome sequence of *Moorella thermoacetica* (f. *Clostridium thermoaceticum*). Environ Microbiol 10 (2008) 2550-73.

[92] F.P. Rosenbaum, A. Poehlein, R. Daniel, and V. Muller, Energy-conserving dimethyl sulfoxide reduction in the acetogenic bacterium *Moorella thermoacetica*. Environ Microbiol (2022).

[93] D.P. Wiesenborn, F.B. Rudolph, and E.T. Papoutsakis, Coenzyme A transferase from *Clostridium acetobutylicum* ATCC 824 and its role in the uptake of acids. Appl Environ Microbiol 55 (1989) 323-9.

謝辞

本研究を遂行するにあたり、ご指導いただきました広島大学統合生命科学研究科生物工学プログラム代謝変換制御学研究室　中島田　豊教授、青井　議輝准教授、加藤　節助教、加藤　淳也特任助教に厚く御礼申し上げます。

また、論文審査に際して貴重な助言とご指導を頂きました生物工学プログラム　秋　庸裕教授、岡村　好子教授に深く感謝いたします。

更に、共同研究者として、ご支援いただきました産業技術総合研究所　松鹿昭則博士、森田　友岳博士、村上　克治博士、藤井　達也博士、和田　圭介博士、岩崎　祐樹博士に深く感謝いたします。

最後に、同じ研究グループとしてご協力いただきました代謝変換制御学研究室の皆様に改めてご御礼申し上げます。

2022 年 9 月